

Structure-based design of MtpB inhibitors that reduce multi-drug-resistant *Mycobacterium tuberculosis* survival and infection burden *in vivo*

¹, §Clare F. Vickers, ², §Ana Silva, ²Ajanta Chakraborty, ²Paulina Fernandez, ⁵Natalia Kurepina, ²Charis Saville, ³Yandi Naranjo, ³Miquel Pons, ⁴Laura S. Schnettger, ⁴Maximiliano G. Gutierrez, ⁵Steven Park, ⁵Barry N. Kreiswith, ⁵David S. Perlin, ¹Eric J. Thomas, ²Jennifer S. Cavet, and ²,*Lydia Tabernero.

Affiliations:

¹The School of Chemistry, University of Manchester, Manchester M13 9PL, UK

²School of Biological Sciences, Faculty of Biology Medicine and Health, University of Manchester, Manchester Academic Health Science Centre, Manchester, M13 9PT, UK.

³ Departament de Química Inorgànica i Orgànica, Universitat de Barcelona, Baldiri Reixac, 10-12, 08028 Barcelona, Spain.

⁴ Host-pathogen interactions in tuberculosis laboratory, The Francis Crick Institute, 1 Midland Road NW1 1AT, London, UK

⁵ Public Health Research Institute, New Jersey Medical School, Rutgers University, 225 Warren Street, Newark, NJ 07103.

§ these authors have contributed equally to the study.

* corresponding author: Lydia Tabernero (Lydia.Tabernero@manchester.ac.uk)

Abstract

Mycobacterium tuberculosis protein-tyrosine-phosphatase B (MtpB) is a secreted virulence factor that subverts antimicrobial activity in the host. We report here the structure-based design of selective MtpB inhibitors that reduce survival of multidrug-resistant tuberculosis strains in macrophages and enhance killing efficacy by first-line antibiotics. Monotherapy with an orally bioavailable MtpB inhibitor reduces infection burden in acute and chronic guinea-pig models and improves the overall pathology. Our findings provide a new paradigm for tuberculosis treatment.

Introduction

Tuberculosis (TB) remains a major health problem and leading cause of death worldwide. Antibiotic resistance is a main obstacle in the cure and eradication of TB, with over half a million new cases of drug-resistant TB per year. More alarming is the increasing number of extensive or untreatable drug-resistant TB cases (WHO TB Report 2017). Critical to the pathogenesis of *Mycobacterium tuberculosis*, the causative agent of TB, is the secretion of virulence factors that subvert the innate immune response and prevent bacterial control by host macrophages^{1, 2}. In this context, anti-virulence drugs targeting the pathogen survival mechanisms may represent an efficient complementary strategy to antibiotics to increase efficacy and assist in clearing the infection. Anti-virulence strategies are now emerging as promising therapies to counterbalance antibiotic resistance in a number of microbial infections including TB^{3, 4, 5, 6, 7}, and yet this is a largely unexploited area in the clinic.

One such virulence factor is the MtpB phosphatase that is secreted into the cytoplasm of host macrophages⁸. MtpB is critical for *M. tuberculosis* intra-macrophage survival and for persistence of the infection in animal models^{9, 10}, and acts by both attenuating the bactericidal immune responses and promoting host cell survival. We report here that selective inhibition of MtpB impairs survival of multi-drug resistant (MDR) TB in human macrophages and reduces infection burden in acute and chronic guinea-pig models. Furthermore, inhibition of MtpB enhances mycobacterial killing by the first-line antibiotics rifampicin (RIF) and isoniazid (INH). Previously we have reported that MtpB dephosphorylates *in vitro* the key signalling lipids phosphatidylinositol 3-

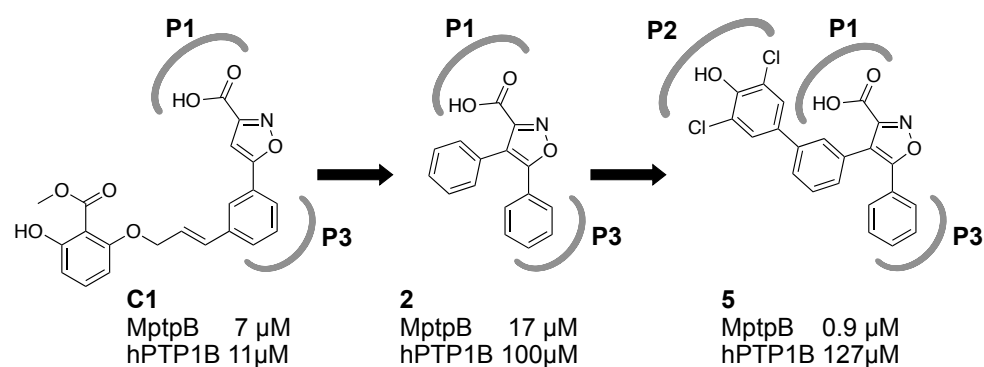
phosphate (PI3P) and phosphatidylinositol 3,5-biphosphate (PI(3,5)P2)¹¹. These lipids control critical steps of phagolysosomal biogenesis and bacterial clearance¹². We hypothesised that inhibition of MptpB activity may thus restore the intrinsic host response compromised by this virulence factor, offering a novel therapeutic mechanism against *M. tuberculosis* infections. Since MptpB is not essential for extracellular growth¹⁰, its inhibition could prove a distinct therapeutic advantage over antibiotics as it would potentially inflict less selective pressure and reduce acquired drug resistance. An additional advantage is that to block the secreted MptpB there is no need for drug delivery across the complex and poorly permeable mycobacterial cell-wall. The lack of a human orthologue also makes MptpB an attractive drug target for specific and selective therapy.

Crucially, we, and others, have demonstrated that MptpB inhibitors impair mycobacterial survival in macrophages^{13,14,15}, supporting our hypothesis. Our initial isoxazole-based MptpB inhibitors displayed modest potency and selectivity¹³. Other reported potent MptpB inhibitors showed little efficacy in animal models¹⁵ indicating that optimisation of both target affinity and pharmacokinetics are needed to develop compounds with *in vivo* efficacy.

We report here the rational structure-based development of our initial **C1** isoxazole inhibitor¹³ to generate a new series of MptpB inhibitors with improved potency, selectivity and cell activity. Furthermore, an analogue from this series showed an excellent pharmacokinetics profile, oral bioavailability and *in vivo* efficacy in guinea pig models of tuberculosis infection.

Results and Discussion

The structure of MptpB¹⁶ has an unusually large active site, with a primary phosphate-binding pocket (P1) and two unique secondary pockets (P2 and P3) not present in human phosphatases. In the crystallographic structure of MptpB with an oxalylamino-methylene-thiophene sulphonamide inhibitor¹⁷, the oxalylamino group binds to P1 whereas the sulphonamide partially occupies P2. Molecular docking of our **C1** inhibitor¹³ indicated that the isoxazole group bonded to P1 and P3, but P2 remained unoccupied (Fig. 1). Our strategy to develop this initial hit used a structure-based rational approach aimed to retain binding at P1 and P3 (isoxazole warhead) whilst exploiting binding at P2 to increase potency and selectivity, see, for example, structures **2** and **5** (Scheme 1, Figure 1).



Scheme 1. Development of the new series of isoxazole-based compounds. The P1/P3 binding isoxazole warhead was used as the starting core. Subsequent addition of a 4-phenyl linker and the dichloro-phenol fragment generated the parent compound **5** providing higher potency and selectivity over human phosphatase PTP1B.

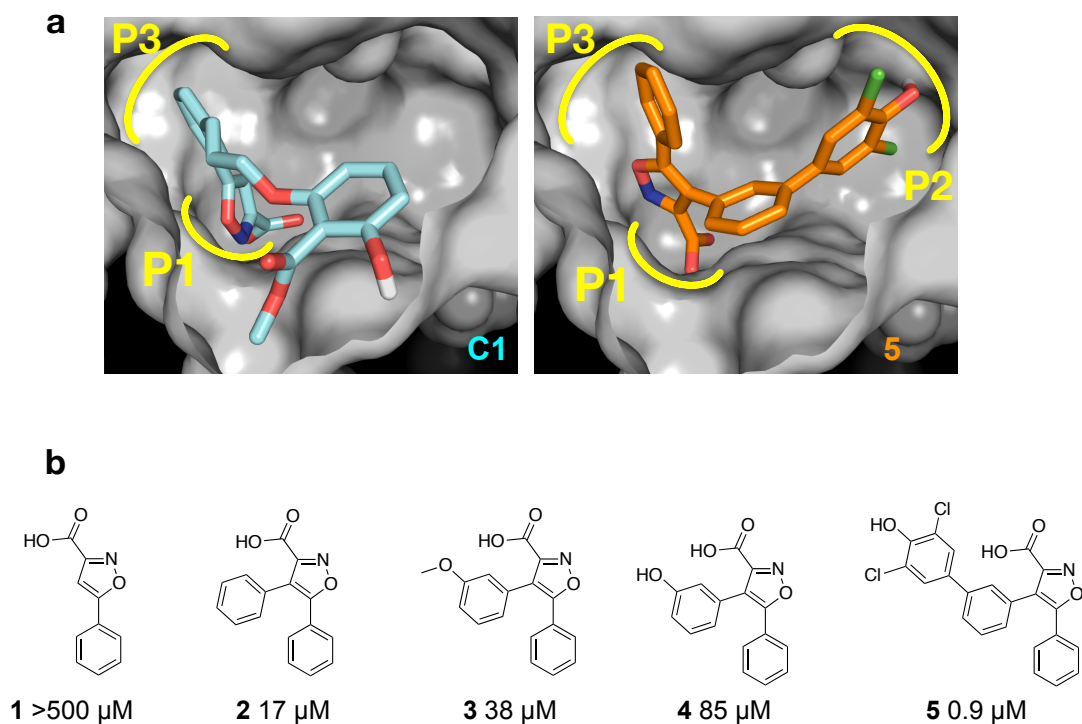
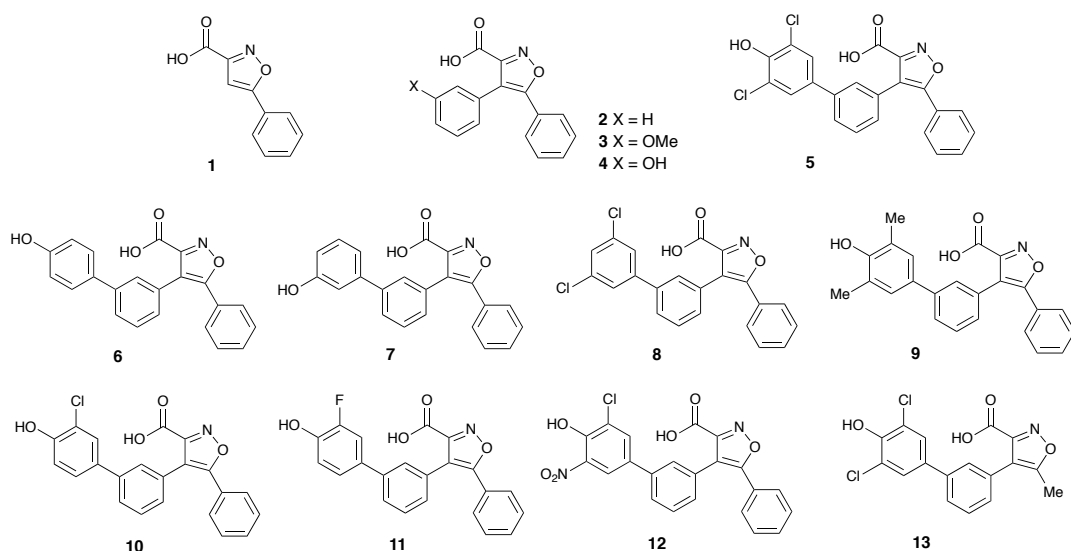


Figure 1. Rational structure-based design of MptpB inhibitors. a) Active site of MptpB with compounds **C1** (cyan)¹³ and **5** (orange) docked. The isoxazole head in **C1** and **5** occupy the P1 pocket (P-loop) and neighbouring P3 pocket, whereas the additional dichloro-phenol group in **5** occupies P2. **b)** The poor activity of the isoxazole head alone and that of the intermediates of the series confirms that binding at P2 is essential to achieve higher potency.

Computational screening of commercial fragment libraries using a genetic based algorithm^{18, 19} and the structure of MptpB¹⁷ identified >300 motifs interacting at P2, providing suitable starting points for the design of a new series of 4,5-diarylisoxazole-3-carboxylic acids (Scheme 2).



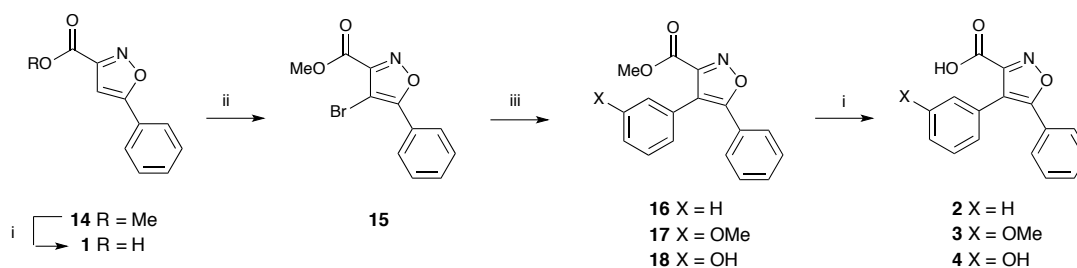
Scheme 2 Isoxazoles identified for synthesis.

Synthesis of 4,5-diarylisoxazole-3-carboxylic acids

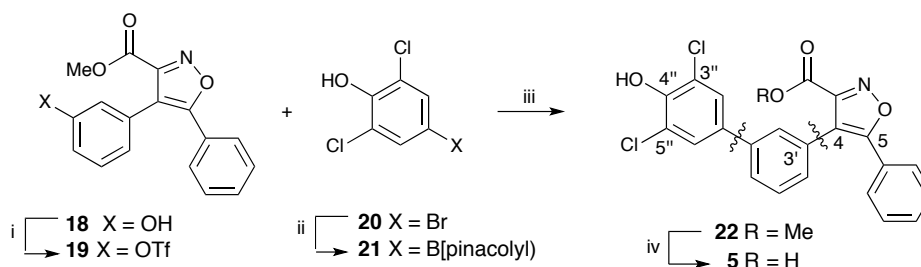
Isoxazoles **1** – **13** were identified for synthesis (Scheme 2). The synthesis of 4,5-diarylisoxazole-3-carboxylic acids **1** – **4** is outlined in Scheme 3. Methyl 5-phenylisoxazole-3-carboxylate **14** is well known^{20, 21} and was synthesized from acetophenone by a slight modification of literature procedures (see experimental). Following bromination of the methyl carboxylate **14**, Suzuki couplings of the bromoisoxazole **15**²² with phenyl-, 3-methoxyphenyl- and 3-hydroxyphenyl-boronic acids gave the 4,5-diarylisoxazole-3-carboxylates **16**²³, **17** and **18**. Saponification of these, and the isoxazolecarboxylate **14**, gave the corresponding carboxylic acids **1** – **4**.

The triflate **19** prepared from the phenol **18** was coupled with the boronate **21**, that was available from 4-bromo-2,6-dichlorophenol **20**, to give the methyl 4,5-

diarylisoxazole-3-carboxylate **22**. This was hydrolysed to give the isoxazole-3-carboxylic acid **5** ready for screening, see Scheme 4.



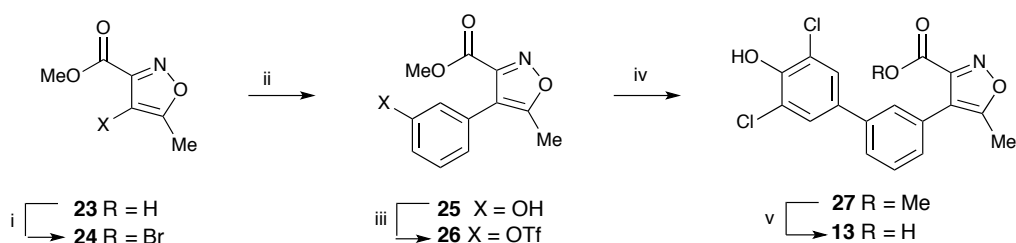
Scheme 3. Synthesis of the 4,5-diarylisoxazole-3-carboxylic acids **1 - 4** Reagents and conditions: i, NaOH, MeOH, THF, rt, 1 h (**1**, 65%; **2**, 60%; **3**, 50%; **4**, 55%); ii, NBS, TFA, heat under reflux 48 h (64%); iii, ArB(OH)₂, Na₂CO₃, DMF, bis(triphenylphosphine)palladium(II) dichloride or Pd(Ph₃P)₄, 90 °C, 1 – 3 h (**16**, 80%; **17**, 42%; **18**, 49%).



Scheme 4. Preparation of the isoxazole-3-carboxylic acid **5** Reagents and conditions: i, (CF₃SO₂)₂O, py., DCM, 0 °C to rt, 90 min (94%); ii, bis(pinacolato)diboron, [1,1'-bis(diphenylphosphino)ferrocene]palladium(II) dichloride, dioxane, 90 °C, 18 h (59%); iii, **19**, **21**, DMF, Na₂CO₃, Pd(PPh₃)₄, 90 °C, 3 h (45%); iv, NaOH, MeOH, rt, 1 h (81%).

The analogous isoxazole-3-carboxylic acids **6 - 12** were similarly obtained from the triflate **19** and the requisite aryl boronic acid or boronate. These were commercially available except that they required the preparation of the isoxazole **12**. This was prepared from the corresponding bromide (see

experimental). Analogous chemistry was used to prepare the 5-methylisoxazole-3-carboxylic acid **13** from the known methyl 4-bromo-5-methylisoxazole **24**, see Scheme 5.



Scheme 5. Preparation of the 5-methylisoxazole-3-carboxylic acid **13** Reagents and conditions: i, NBS, TFA, 0 °C, heat under reflux, 16 h; ii, ArB(OH)₂, aq. NaHCO₃, DMF, Pd(Ph₃P)₂Cl₂, 90 °C, 5 h (28%); iii, (CF₃SO₂)₂O, py., DCM, 0 °C to rt, 6 h (66%); iv, **21**, Pd(Ph₃P)₄, DMF, 90 °C, 3 h; v, NaOH, MeOH, 0 °C, 1 h (65%).

Activity of the 4,5-diarylisoxazole-3-carboxylic acids and biochemical validation

The initial isoxazole fragment alone **1** showed very poor inhibition, but the introduction of a phenyl ring at the 4-position reduced the IC₅₀ from >500 μM **1** to 17 μM **2**. Extending the aromatic ring with a di-chlorophenol fragment, identified in the computational screen, afforded a further reduction to 0.9 μM **5**. Improved binding for the new compounds was accompanied with increased selectivity over the human phosphatase hPTP1B from 1.6-fold for compound **C1** to 5.9-fold for compound **2** and 141-fold for compound **5** (Fig. 1b), supporting the notion that binding at P2 is critical for selectivity.

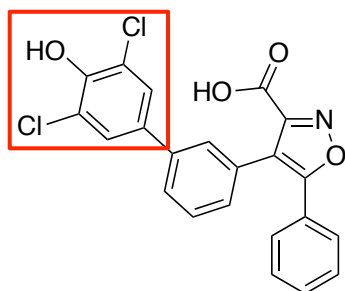
Computational docking analysis of the new series of compounds showed a good

correlation between the estimated free energy of binding and the experimental activity (Supplementary Table 1). Molecular docking confirmed that additional binding at P2 was responsible for the significant increase in potency of **5** compared to compounds **2 - 4**. Subsequently, we explored variations of the dichlorophenol fragment substituents in the derivatives **6 - 12** (Table 1).

The double and triple substituted aromatic groups showed similar IC₅₀ to **5**. The introduction of the NO₂ group at the *meta*-position of the phenyl ring **12** increased potency by 50 % with respect to **5** resulting in an IC₅₀ of 0.4 μM, and afforded an excellent selectivity over human phosphatases (900-fold for PTP1B) and the *M. tuberculosis* phosphatase MptpA (Table 1).

Our models suggested that the *para*-OH group of the phenyl ring (P2 head), could form hydrogen bonds with the Oε1 of E129 (Fig. 2a) and that the *meta*-NO₂ group in **12** could form additional interactions with R136 or H94 thus explaining its increased potency. Mutational analysis of the P2 pocket residues validated this mode of binding. Mutations of E129 to alanine showed a 2 to 5-fold decrease in inhibition (Fig. 2b), while mutation of H94 or R136 had a milder effect (~2-fold decrease).

Table 1. Inhibitory activity of the 4,5-diarylisoazole-3-carboxylic acids and selectivity over *M. tuberculosis* and human phosphatases. Scaffold of the new series of isoxazole-based compounds is shown at the top. Substitutions of the dichloro-phenol head (red square) were explored during development of compound 5. Activities (IC_{50} values in μM) towards *M. tuberculosis* MptpB, MptpA, and human PTP1B and Vaccinia H1-related (VHR) phosphatases are shown.



P2 Head	Compound	IC_{50} (μM)			
		MptpB	MptpA	hPTP1B	hVHR
	5	0.92 ± 0.03	33.7 ± 0.6	127 ± 9	10.5 ± 0.5
	6	2.8 ± 0.3	74 ± 1.0	>100	54.0 ± 4.6
	7	2.3 ± 0.7	95 ± 5.0	>100	59 ± 1.0
	8	1.2 ± 0.3	6.5 ± 0.3	48 ± 3	12.3 ± 1.0
	9	1.1 ± 0.1	36 ± 2.0	>100	23.2 ± 0.3
	10	0.9 ± 0.1	23.5 ± 0.5	213 ± 29	18.7 ± 1.5
	11	1.5 ± 0.1	35.3 ± 3.1	>100	40.2 ± 1.3
	12	0.40 ± 0.05	30.2 ± 1.4	313 ± 29	13.0 ± 1.0

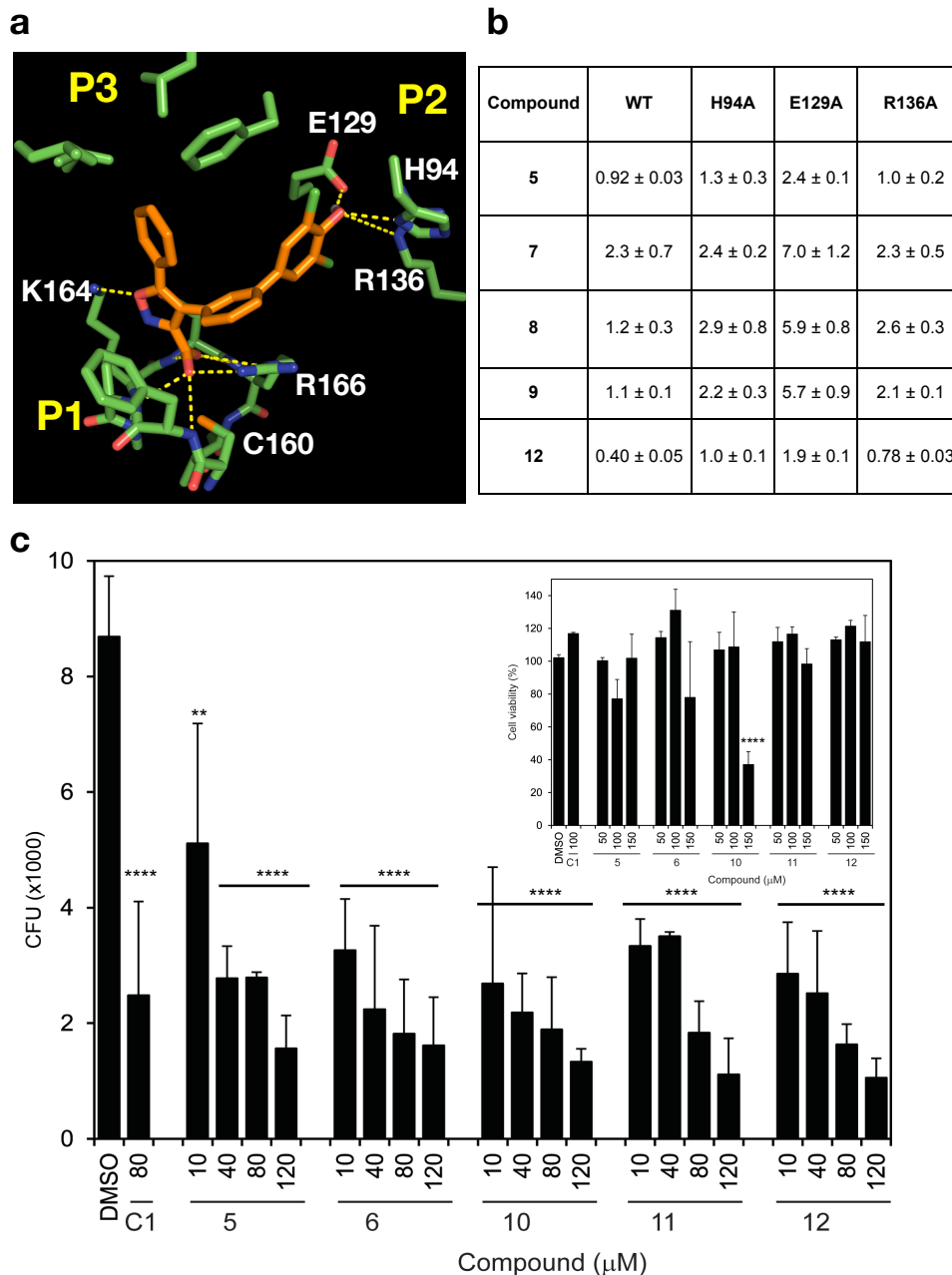


Figure 2. Binding at the P2 pocket is important for the efficacy of the new series of MptpB inhibitors. **a)** Mode of binding of the representative compound 5 into the active site of MptpB, as suggested from the molecular docking. **b)** Mutation of key interacting residues at the P2 pocket resulted in a loss of 2-5 fold the IC_{50} values (μM). **c)** Cell activity of the new series results in substantial (81-87%) reduction in the mycobacterial (BCG) burden of infected mouse macrophages (J774) 72 hours post infection, compared to DMSO-treated macrophages. Reduction in bacterial burden is already observed at 24 hours post-infection (Suppl. Fig.2). Plots represent the average CFUs (+SEM) per well (from a 96-well plate, see methods for details) of at least three independent experiments, with statistical significance relative to the control (DMSO treated)

established using one-way ANOVA, Dunnett's test (**** p -value < 0.0001, ** p =0.012). Inset shows viability of treated macrophages.

The new MtpB inhibitors reduce mycobacterial burden in macrophage infections

Next we tested the efficacy of the new compounds in reducing mycobacterial survival in macrophage infections. The new series of compounds showed dose-dependent efficacy in reducing intracellular mycobacterial (BCG) burden in mouse macrophages (J774) up to 87% after 72h of infection compared to control (DMSO treated) (Fig. 2c). These findings are consistent with MtpB inhibition assisting bacterial clearance in host macrophages, even in the absence of INF- γ activation (see methods). The new compounds show increased efficacy at 80 μ M (except for **5**) compared to our initial **C1** isoxazole inhibitor, thus correlating with the higher potency of the new series. Toxicity of the new compounds is low as shown in the cell survival assays (Fig 2c inset), with only compound **10** showing a substantial effect (>23% reduction) on cell viability at > 100 μ M doses.

The new series of compounds displayed moderate permeability and lipophilicity (logD), good solubility, they were stable in plasma with moderate clearance in human liver microsomes, and high plasma protein binding (Suppl. Table 2). They also showed poor *in vivo* pharmacological properties in guinea-pigs, with a bioavailability below 13% (Table 2). We then replaced the phenyl ring at position 5 of the isoxazole by a methyl group to reduce the bulk and number of rings in the compound, generating compound **13**. The potency of compound **13**,

at 3 μ M, was lower than the best of the parent series of inhibitors **5** and **12** (by 3-7 fold), possibly due to reduced hydrophobic interactions at the P3 pocket. However, compound **13** showed very good kinetic solubility (200 μ M), and a good PAMPA value (78.1 nM/s) suggesting a potential good cell penetration, despite showing a higher lipophilicity than the parent series (logD 4) (see Supplementary material for details). Importantly, compound **13** displayed improved pharmacological properties, it is orally bioavailable and has an excellent pharmacokinetic profile (Table 2), therefore it was selected for further evaluation of its cell activity and efficacy in animal models of infection.

Table 2. Pharmacokinetic parameters for MptpB inhibitors. Compounds 3, 8, 9 and 13 were tested in guinea-pigs to determine their PK profile. C_{max} was observed at 0.5 hr after IP (intraperitoneal) dosing and at 0.25 hr after PO (oral) dosing.

Compound	13 (lead)		5		8		9	
	Guinea pig		Guinea pig		Guinea pig		Guinea pig	
Route	IP	Oral	IP	Oral	IP	Oral	IP	Oral
Dose (mg/kg)	4	8	2.5	5	1.25	3.5	2.5	5
C_{max} (ng/mL)	31519	111099	3714	BLQ	746	BLQ	197	BLQ
$t_{1/2}$ (hr)	1.4	5.1	0.7	BLQ	1.3	BLQ	1.4	BLQ
AUC_{inf} (ng.hr/mL)	71854	230407	4968	BLQ	1742	BLQ	399	BLQ
Bioavailability		156%*		<4%		<13%		<2.5%

**High bioavailability may be due to prolonged absorption after the oral dose limiting the rate of elimination; BLQ, below limit of quantification.*

MptpB inhibitors reduce survival of multidrug-resistant strains in macrophages and enhance killing by first-line antibiotics

Investigation of compound **13** demonstrated that it also exhibits dose-dependent efficacy in reducing intracellular mycobacterial (BCG) burden in mouse macrophages (J774) up to 84% (Fig. 3b), yet it does not affect extracellular bacterial growth (Fig. 3c), thus confirming that inhibition exclusively targets intracellular mycobacteria, as expected. Critically, treatment with compound **13** also reduces the intracellular mycobacterial burden in human macrophages (THP1), up to 63% when using a drug-susceptible *M. tuberculosis* strain (H37Rv), or up to 74% when using a MDR strain (Beijing-“W”) (Fig. 3d). A similar effect was observed for the initial **C1** compound (Supplementary Figure 1) demonstrating that efficacy in reducing MDR-TB survival is a general quality of MptpB inhibitors.

To test whether compound **13** is compatible with first-line TB drugs, isoniazid (INH) and rifampicin (RIF), we determined doses of these antibiotics that caused < 25% reduction in the bacterial burden of macrophages (0.1 µg/ml for INH and 0.3 µg/ml for RIF, Fig. 3e). We then used these doses of INH and RIF in combination with a low dose, 5 µM, of compound **13**. The combination resulted in > 93% reduction in bacterial burden (Fig. 3e). Thus, treatment in combination with compound **13** enhances killing by current anti-tubercular drugs. This is an important finding since tuberculosis treatments rely on drug combination therapies to clear the infection.

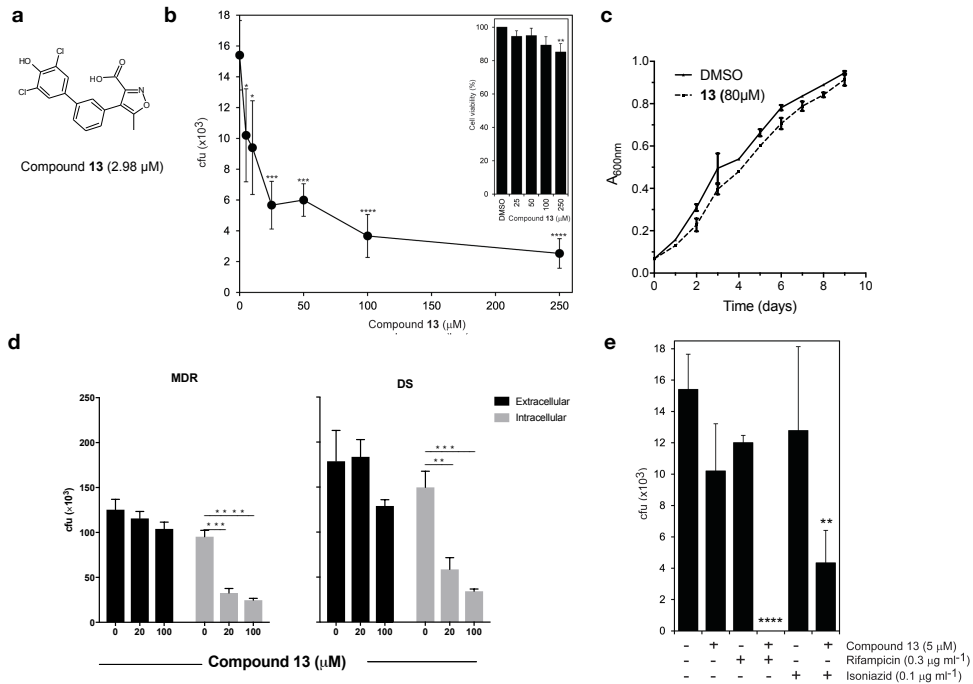


Figure 3. Compound 13 reduces intracellular bacterial burden of H37Rv and MDR-TB in macrophage infections. **a)** Structure of compound 13. **b)** Effect of dose-dependent treatment with compound 13 on mycobacterial burden (BCG) in infected mouse macrophages (J774) at 72 hours post infection (**** $p < 0.0001$, *** $p < 0.0004$, * $p < 0.04$ by one-way ANOVA, Dunnett's test). Inset shows macrophage viability upon treatment with 13 (** $p=0.01$). **c)** Extracellular growth of BCG is not affected by treatment with compound 13 (80 μM) respect to DMSO control. **d)** Treatment with compound 13 (20 or 100 μM) reduces intracellular survival of an MDR strain (Beijing-W) and of the drug-susceptible *M. tuberculosis* H37Rv strain in human THP1 macrophages (grey). Controls on the effect on extracellular bacterial growth are shown (black), ** $p=0.0021$; *** $p=0.0002$, **** $p<0.0001$ by unpaired t test). **e)** Treatment with compound 13 increases the antibacterial activities of RIF and INH antibiotics in infected macrophages (BCG in J774 mouse macrophages, **** $p < 0.0001$, ** $p=0.0017$, by one-way ANOVA, Dunnett's test). **d** and **e)** data are the mean CFUs at 72 hours post infection of at least three biological replicates (+SEM). Limit of detection is < 10 cfu.

MptpB inhibition alters phagosomal phosphoinositide-3-phosphate dynamics during infection

MtpB dephosphorylates PI3P and PI(3,5)P₂ *in vitro*¹¹, two important anchors of Rab proteins that drive phagosomal maturation and clearance of infection. However, we do not know its effect on cellular PI dynamics. We tested if compound **13** affected PI3P dynamics on *M. tuberculosis*-phagosomes. For that, we monitored PI3P localisation by live-cell imaging in macrophages expressing a fluorescent PI3P-binding module (FYVE2X-EGFP) after infection with fluorescently labelled *M. tuberculosis* H37Rv²⁴. PI3P associated with *M. tuberculosis*-phagosomes immediately after infection, but PI3P signal decreased rapidly after 2-4 minutes as previously reported²⁴. However, in the **13**-treated macrophages, the peak of PI3P was prolonged up to 12 minutes (Fig. 4). The data indicate that MtpB inhibition extends the presence of PI3P and its association with *M. tuberculosis*-phagosomes, suggesting a role for MtpB in host phosphoinositide metabolism as hypothesised from its *in vitro* activity¹¹.

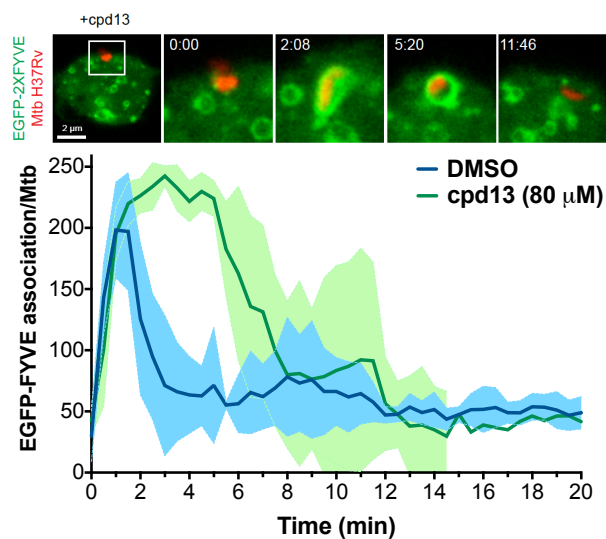


Figure 4. MptpB inhibition alters phagosomal PI3P dynamics. Spatio-temporal dynamics of PI3P (as visualised by expression of EGFP-FYVE) on *M. tuberculosis* containing phagosomes (top figure). The plot shows the quantitative analysis of the association of EGFP-FYVE to PI3P at the phagosomal membrane, during the first 20 minutes of phagocytosis (data from 3 independent experiments). Treatment with **13** extends the peak of PI3P up to 12 min. compared to the rapid decay of PI3P peak in the untreated phagosomes (DMSO control). DMSO, control for untreated macrophages (RAW264.7); cpd **13**, macrophages treated with compound **13**.

Monotherapy with an orally bioavailable MptpB inhibitor reduces infection burden in acute and chronic guinea-pig models

In vivo profiling of compound **13** showed high exposure (C_{max} 112 μ g/ml, AUC 230 μ g.hr/ml), long half-life ($t_{1/2}$ 5 hours), good oral availability and relevant tissue distribution in guinea-pigs, upon parental and oral dosing (Table 2 and Supplementary Fig. 3), making it suitable for efficacy studies in animal models of infection. Tolerability studies with **13** at 50, or 100 mg/kg (dosing once daily for 7 days) showed no adverse drug effects and weight increases of >5% was

observed in all animals during the tolerability trial.

Compound **13** was then assessed for efficacy as monotherapy in the *acute* and *chronic* guinea-pig models of TB infection. For the acute infection, animals were infected with 96 CFU (avg. \pm 27 SEM), and after 24hrs, orally dosed once daily with compound **13** for 4 weeks. Treatment resulted in a 0.9 log reduction of bacterial burden in the lungs relative to vehicle. For the chronic infection, guinea pigs were infected with 63 CFU (avg. \pm 18 SEM), and treatments were orally administered daily for 4 weeks starting at 28 days post infection. Treatment with compound **13** resulted in at least 1 log reduction in bacterial burden in lungs and spleens (Fig. 5a and Supplementary Table 3).

Pathological differences were observed between **13** and vehicle treated groups in both lungs and spleens (Fig 5b-e) from both the acute and chronic infection studies. Although the total number of tubercles were similar in both **13** and vehicle treated animals, larger tubercles were consistently present in all vehicle group. Overall, less damage to the spleens and lungs were observed in the **13** treated group relative to the vehicle only group.

Inspection of the lungs and spleens after 56 days of infection revealed visible necrotic lesions ranging from \sim 1 to 4 mm, with more consolidation observed in the vehicle group than in the compound **13** treated group, and with organs presenting up to 19% increase in weight respect to the **13** treated group (Suppl. Table 4). The histopathological analysis of the vehicle treated lungs and spleens displayed large and diffuse confluent granulomas with necrotising cores and inflammation throughout the parenchyma, pathology typically associated with a chronic infection. The compound **13** treated lungs and spleens showed an

improvement in the pathology with fewer smaller lesions and reduced inflammation both in lungs and spleens (Fig. 5e).

These results provide proof-of-concept that MptpB inhibitors, used as monotherapy, can be effective in controlling TB infection in animal models, despite not having direct bactericidal activity. Particularly significant for clinical applications is the efficacy and improved pathology observed in the chronic model because guinea-pigs develop a similar immunopathology and inflammatory response to the infection as in humans, forming granulomas that contain persistent bacteria ^{25, 26}.

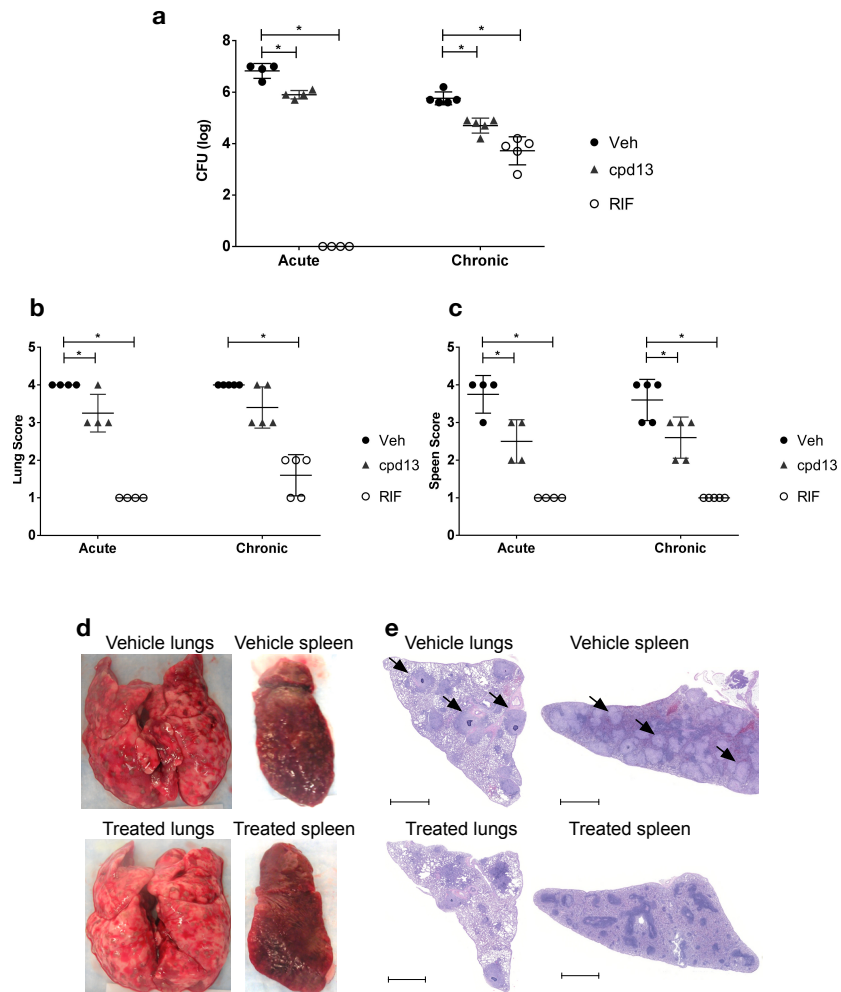


Figure 5. MptpB inhibition reduces bacterial burden in animal models and improves pathology. **a)** Efficacy of monotherapy treatment with **13** for 28 days in the acute and chronic guinea-pig models of TB (female Hartley Duncan). Treatment was with **13** (100 mg/kg) or RIF (50mg/kg) orally administered once daily; VEH, vehicle control. Bars represent the mean value (\pm SEM) of CFUs from 4-5 animals. Statistical significance is indicated (* $p < 0.05$ by one-way ANOVA, Dunnett's test). **b)** and **c)** Gross pathological scoring of the TB infected guinea-pig lungs (**b**) and spleens (**c**) based on Jain et al. ²⁷ The lungs and spleen from individual animals were given a score from 1 to 4 based on the number and size of tubercles, level of involvement, inflammation and necrosis. Bars represent the mean value (\pm SEM) of CFUs from 4-5 animals. Statistical significance is indicated (* $p < 0.05$ by one-way ANOVA, Dunnett's test). **d)** Representative images of tissues at 56 days post infection (chronic model) showing reduction of the number granuloma in the compound **13** treated lungs and spleen. **e)** Representative histopathological images from lungs and spleens at 56 days post infection from (chronic model). Lungs and Spleens fixed in neutral buffer formalin were sectioned (5 micron) and stained with hematoxylin and eosin (H&E) and imaged at 10x magnification. Vehicle treated lungs and spleen show an increased presence of granulomatous infiltration (black arrows) and pathologic damage relative to compound **13** treated lungs and spleen. Bars represent 2 mm.

Conclusions

In summary, our structure-guided drug development approach, exploiting unique features in the MptpB structure, has delivered an orally bioavailable compound with excellent therapeutic properties. We have demonstrated that MptpB inhibitors are selective, effective against MDR-TB and that they increase the intracellular killing efficacy of first line antibiotics RIF and INH, indicating their suitability for combination therapies. Notably, reduction of intracellular survival occurs in the absence of macrophage pre-activation with IFN γ , suggesting that this strategy may be particularly advantageous when impaired macrophage activation fails to control the infection (i.e. immuno-compromised patients).

Importantly, our lead compound showed efficacy in reducing bacterial burden in a clinically-relevant guinea-pig model of infection, as well as improvement in the pathology of lungs and spleen. This is also consistent with the enhanced pathology and reduced inflammation observed when the *mptpB* gene is mutated⁹. This is the first proof of concept that MptpB inhibitors, used as monotherapy, can significantly reduce infection burden. A previous study¹⁵ showed a mild effect (< 0.5 log reduction) when both MptpA and MptpB inhibitors were added to a cocktail of three first-line antibiotics, isoniazid– rifampicin–pyrazinamide (HRZ), effectively a 5-drug combination. However, there was no effect on bacterial burden when only MptpA or MptpB inhibitors were added to the HRZ cocktail. No data were presented on monotherapy treatments with either MptpA or MptpB inhibitors, thus no direct comparison can be made with our results.

Renewed interest in developing anti-virulence agents for TB treatment (reviewed in^{3, 4, 5, 6,7}) makes this study timely. Furthermore, MptpB inhibitors could be developed into broad-spectrum anti-virulence drugs, as MptpB orthologues are present in more than 50 human pathogens including *C. difficile*, *E. faecalis*, *K. pneumoniae*, *Yersinia spp* and *L. monocytogenes*^{28,29}.

Anti-virulence drugs hold great promise for the management of TB infections. The current challenges in eradicating TB include: prevention with the existing BCG vaccine has limited efficacy; standard treatments with antibiotics are long, complex and chronic drug exposure over a prolonged period is linked to development of drug resistance; and host-directed therapies are difficult to control because they are patient-dependent. Anti-virulence agents offer advantages to overcome these challenges because their action is independent of the host fitness and they have the potential to limit drug resistance. Our findings suggest that MptpB inhibition offers a new paradigm for TB therapy with the potential to treat MDR-TB, improve antibiotic efficacy and overall pathology.

Experimental Methods

Synthetic Chemistry

General experimental details

All reactions were carried out under an atmosphere of dry nitrogen unless otherwise stated. Low-resolution mass spectra were recorded on a Micromass Trio 200 spectrometer using electron impact (EI) ionisation or electrospray in positive (ES⁺) or negative modes (ES⁻). High-resolution mass spectra were recorded on a Kratos Concept IS spectrometer. Infrared spectra were recorded on a Genesis FTIR as evaporated films on sodium chloride plates. Proton NMR spectra (¹H NMR) and carbon NMR spectra (¹³C NMR) were recorded on Bruker (500 MHz), Varian Unity 500 (500 MHz), Varian INOVA 400 (400 MHz) or Varian INOVA Unity 300 (300 MHz) spectrometers. Residual non-deuterated solvent was used as internal standard. Chemical shifts (δ_{H} and δ_{C}) are quoted in parts per million (ppm) downfield from tetramethylsilane (TMS).

Flash column chromatography was carried out using silica gel 60H from Merck. Light petroleum refers to the fraction that boils between 40 °C and 60 °C and was distilled prior to use. Ether refers to diethyl ether that was used without further purification. Tetrahydrofuran was dried over sodium/benzophenone and was distilled under a nitrogen atmosphere. DCM was dried over calcium hydride and distilled under an atmosphere of nitrogen. All other reagents and solvents were used as purchased unless otherwise stated. The purity of compounds submitted for screening was determined to be greater than 95% by HPLC (see supplementary data for copies of the HPLC traces)

5-Phenylisoxazole-3-carboxylic acid (1); standard procedure ^{30 31}

Aqueous sodium hydroxide (2 M, 2.7 mL, 5.4 mmol) was added to methyl 5-phenylisoxazole-3-carboxylate **14** (219 mg, 1.08 mmol) in MeOH:THF (1:1 v/v, 60 mL) at rt and the mixture was stirred for 1 hour. Water was added (60 mL) and the mixture acidified to pH 1 using aqueous hydrogen chloride (2 M) then concentrated under reduced pressure to give a slurry that was extracted with EtOAc (3 × 60 mL). The organic extracts were dried (NaSO₄) and concentrated under reduced pressure to give an off-white solid that was recrystallised (light petroleum:EtOAc, 100:1 v/v) to give the title compound **1** as a white solid (132 mg, 0.7 mmol, 65%); mp: 162.8 – 163.8 °C (lit. ³¹ 160-161 °C); TLC (light petroleum:EtOAc, 50:50 v/v, with 0.1% TFA): R_f = 0.3; HPLC (silica, EtOAc with 0.1 % TFA): retention time 3.27 min, 100 %; ¹H NMR (500 MHz, DMSO-*d*₆): δ 14.13 (br. s, 1H), 7.96 (d, *J* 8.0 Hz, 2H), 7.59-7.54 (m, 3 H), 7.44 (s, 1H); ¹³C NMR (125 MHz, DMSO-*d*₆): δ 170.8, 160.9, 157.8, 130.9, 129.3, 126.2, 125.8, 100.9; IR (film): 3126, 3055, 2611, 2512, 1703, 1474, 1445, 1261, 995, 914, 820, 760, 686 cm⁻¹.

4,5-Diphenylisoxazole-3-carboxylic acid (2) ²³

Following the procedure outlined for the preparation of carboxylic acid **1**, methyl 4,5-diphenylisoxazole-3-carboxylate **16** (90 mg, 0.32 mmol) in MeOH:THF (1:1 v/v, 6 mL) and aqueous sodium hydroxide (2 M, 0.8 mL, 1.6 mmol), after recrystallisation (light petroleum:EtOAc, 100:1 v/v) gave the title compound **2** as a white solid (51 mg, 0.2 mmol, 60%); mp: 134.5-135.3 °C; TLC (light petroleum:EtOAc, 50:50 v/v with 0.1% TFA): R_f = 0.36; HPLC (silica, EtOAc with

0.1 % TFA): retention time 3.18 min, 100 %; ^1H NMR (500 MHz, $\text{DMSO-}d_6$): δ 13.65 (br. s, 1H), 7.51 - 7.32 (m, 10H); ^{13}C NMR (125 MHz, $\text{DMSO-}d_6$): δ 177.9, 161.0, 151.8, 130.0, 129.1, 128.6, 128.4, 126.6, 116.2; IR (film): 3058, 1711, 1429, 1225, 968, 770, 693 cm^{-1} ; LRMS (m/z , ES^-): 220 ($[\text{M} - 45]^-$, 100%); HRMS (m/z): $[\text{M} + \text{H}]^+$, calcd. for $\text{C}_{16}\text{H}_{12}\text{NO}_3$, 266.0812; found, 266.0817.

4-(3-Methoxyphenyl)-5-phenylisoxazole-3-carboxylic acid (3)

Following the procedure outlined for the preparation of carboxylic acid **1**, 4-(3-methoxyphenyl)-5-phenylisoxazole-3-carboxylate **17** (100 mg, 0.32 mmol) in $\text{MeOH}:\text{THF}$ (1:1 v/v, 6 mL) and aqueous sodium hydroxide (2 M, 0.8 mL, 1.6 mmol), after recrystallisation ($\text{MeOH}:\text{H}_2\text{O}$, 50:1 v/v) gave the *title compound* **3** as a white solid (47 mg, 0.16 mmol, 50%); mp: 162.5-163.5 $^\circ\text{C}$; TLC (light petroleum:EtOAc, 50:50 v/v with 0.1% TFA): $R_f = 0.25$; HPLC (silica, EtOAc with 0.1 % TFA): retention time 3.20 min, 100 %; ^1H NMR (500 MHz, $\text{DMSO-}d_6$): δ 13.94 (br. s, 1H), 7.49-7.42 (m, 5H), 7.35 (t, J 8.0 Hz, 1H), 7.01 (dd, J 2.0, 8.0 Hz, 1H), 6.95 (m, 1H), 6.91 (d, J 7.5 Hz, 1H), 3.73 (s, 3H); ^{13}C NMR (125 MHz, $\text{DMSO-}d_6$): δ 166.0, 160.9, 159.2, 156.3, 130.6, 130.2, 129.7, 129.0, 126.7, 126.4, 122.2, 115.9, 115.7, 113.8, 55.1; IR (film): 3154, 1727, 1621, 1580, 1439, 1276, 1227, 1189, 1095, 1042, 1008, 966, 878, 826, 805, 768, 689 cm^{-1} ; LRMS (m/z , ES^-): 250 ($[\text{M} - 45]^-$, 100%); HRMS (m/z , ES^-): $[\text{M} - \text{CO}_2\text{H}]^-$ calcd. for $\text{C}_{16}\text{H}_{12}\text{NO}_2$, 250.0873; found, 250.0861.

4-(3-Hydroxyphenyl)-5-phenylisoxazole-3-carboxylic acid (4)

Following the procedure outlined for the preparation of carboxylic acid **1**, methyl 4-(3-hydroxyphenyl)-5-phenylisoxazole-3-carboxylate **18** (150 mg, 0.52 mmol) in MeOH:THF (1:1 v/v, 10 mL) and aqueous sodium hydroxide (2 M, 1.5 mL, 3 mmol), after recrystallisation (MeOH:H₂O, 50:1 v/v) gave the *title compound* **4** as a white solid (80 mg, 0.29 mmol, 55%); TLC (light petroleum:EtOAc, 50:50 v/v with 0.1% TFA): R_f = 0.5; HPLC (silica, EtOAc with 0.1 % TFA): retention time 3.22 min, 100 %; ¹H NMR (500 MHz, DMSO-*d*₆): δ 14.04 (br. s, 1H), 9.56 (s, 1H), 7.49-7.41 (m, 5H), 7.22 (t, *J* 8.0 Hz, 1H), 6.81 (d, *J* 7.5 Hz, 1H), 6.75-6.72 (m, 2H); IR (film): 3468, 3243, 3064, 1722, 1629, 1583, 1474, 1444, 1331, 1228, 1176, 971, 867, 795, 766, 687 cm⁻¹; LRMS (*m/z*, ES⁺): 282 ([M + 1]⁺, 100%); HRMS (*m/z*, ES⁺): [M + H]⁺ calcd. for C₁₆H₁₂NO₄, 282.0761; found, 282.0753.

4-(3',5'-Dichloro-4'-hydroxy-3-biphenyl)-5-phenylisoxazole-3-carboxylic acid (5)

Following the procedure outlined for the preparation of carboxylic acid **1**, methyl 4-(3',5'-dichloro-4'-hydroxy-3-biphenyl)-5-phenylisoxazole-3-carboxylate **22** (900 mg, 2.04 mmol) in MeOH:THF (25 mL, 4:1 v/v) and aqueous sodium hydroxide (2 M, 5.11 mL, 10.2 mmol), after recrystallisation (light petroleum:EtOAc, 10:1 v/v) gave the *title compound* **5** as a white solid (700 mg, 1.65 mmol, 81%); mp: 187.5-188.0 °C; TLC (light petroleum:EtOAc, 50:50 v/v with 0.1% TFA): R_f = 0.5; HPLC (silica, EtOAc with 0.1 % TFA): retention time 2.79 min, 100 %; ¹H NMR (500 MHz, DMSO-*d*₆): δ 14.02 (br. s, 1H), 10.35 (s, 1H) and 7.75-7.32 (m, 11H); ¹³C NMR (125 MHz, DMSO-*d*₆): δ 166.3, 160.9, 156.2, 148.6, 137.5, 132.4, 130.6, 129.6, 129.2, 129.0, 128.1, 126.8, 126.6, 126.5, 126.3,

122.8, 116.0; IR (film): 3056, 1717, 1468, 1430, 1291, 1161, 1024, 868, 794, 768, 691 cm^{-1} ; LRMS (m/z , ES⁻): 426 ([M - 1]⁻, 6%), 424 ([M - 1]⁻, 8), 382 ([M - 45]⁻, 65), 380 ([M - 45]⁻, 100); HRMS (m/z , ES⁻): [M - H]⁻ calcd. for $\text{C}_{22}\text{H}_{12}\text{NO}_4^{35}\text{Cl}_2$, 424.0148; found, 424.0154.

4-(4'-Hydroxy-3-biphenyl)-5-phenylisoxazole-3-carboxylic acid (6)

Following the procedure outlined for the preparation of the methyl 4-biphenylisoxazole-3-carboxylate **22**, the aryl triflate **19** (300 mg, 0.7 mmol) and 4-hydroxyphenylboronic acid (107 mg, 0.77 mmol) in DMF (7 mL) together with $\text{Pd}(\text{PPh}_3)_4$ (8 mg, 0.007 mmol), after repeated chromatography (Et_2O :light petroleum, 20:80 - 40:60 v/v, then with DCM) gave methyl 4-(4'-hydroxy-3-biphenyl)-5-phenylisoxazole-3-carboxylate as a white solid (159 mg, 0.427 mmol, 61%); mp: 62.7-63.5 °C; TLC (Et_2O :light petroleum, 40:60 v/v): R_f = 0.14; ^1H NMR (500 MHz, CDCl_3): δ 7.61-7.57 (m, 3H), 7.54 (s, 1H), 7.48 (t, J 7.5 Hz, 1H), 7.43 (d, J 9.0 Hz, 2H), 7.39 (d, J 7.5 Hz, 1H), 7.36-7.33 (m, 2H), 7.29 (d, J 7.5 Hz, 1H) 6.89 (d, J 8.5 Hz, 2H), 5.88 (s, 1H), 3.90 (s, 3H); ^{13}C NMR (125 MHz, CDCl_3): δ 167.4, 160.6, 155.7, 155.0, 141.3, 132.9, 130.5, 129.2, 129.1, 128.9, 128.5, 128.4, 128.3, 127.1, 126.9, 126.8, 116.8, 115.8, 52.9; IR (film): 3374, 1741, 1612, 1519, 1445, 1335, 1221, 1175, 1103, 1018, 838, 770, 694 cm^{-1} ; LRMS (m/z , ES⁻): 370 ([M - 1]⁻, 100%); HRMS (m/z , ES⁺): [M + H]⁺ calcd. for $\text{C}_{23}\text{H}_{18}\text{NO}_4$, 372.1231; found, 372.1223.

Following the procedure outlined for the preparation of the carboxylic acid **1**, methyl 4-(4'-hydroxy-3-biphenyl)-5-phenylisoxazole-3-carboxylate (160 mg, 0.43 mmol) in MeOH (4 mL) and aqueous sodium hydroxide (2 M, 1.1 mL, 2.15 mmol), after recrystallisation (light petroleum:EtOAc, 100:1 v/v), gave the

title compound 6 as a white solid (90 mg, 0.25 mmol, 59%); mp: 186.0-187.3 °C; TLC (light petroleum:EtOAc, 50:50 v/v with 0.1% TFA): R_f = 0.49; HPLC (silica, EtOAc with 0.1 % TFA): retention time 3.23 min, 100 %; ^1H NMR (400 MHz, DMSO- d_6): δ 13.99 (br. s, 1H), 9.60 (s, 1H), 7.67-7.41 (m, 10H), 7.25 (d, J 7.5 Hz, 1H), 6.83 (d, J 8.5 Hz, 2H); ^{13}C NMR (100 MHz, DMSO- d_6): δ 166.2, 161.1, 157.4, 156.3, 140.4, 130.7, 130.2, 129.4, 129.2, 129.1, 128.0, 127.8, 127.6, 126.8, 126.5, 126.0, 116.2, 115.8; IR (film): 3058, 1754, 1655, 1612, 1545, 1512, 1441, 1222, 1177, 836, 803, 760 cm^{-1} .

4-(3'-Hydroxy-3-biphenyl)-5-phenylisoxazole-3-carboxylic acid (7)

Following the procedure outlined for the preparation of the methyl 4-biphenylisoxazole-3-carboxylate **22**, the aryl triflate **19** (300 mg, 0.7 mmol) and 3-hydroxyphenylboronic acid (107 mg, 0.77 mmol) in DMF (7 mL) together with Pd(PPh₃)₄ (8 mg, 0.007 mmol), after repeated chromatography (Et₂O:light petroleum, 20:80 – 40:60 v/v, then with DCM) gave methyl 4-(3'-hydroxy-3-biphenyl)-5-phenylisoxazole-3-carboxylate as a white solid (50 mg, 0.135 mmol, 19%); mp: 59.0-59.6 °C; TLC (Et₂O:light petroleum, 40:60 v/v): R_f = 0.14; ^1H NMR (300 MHz, CDCl₃): δ 7.54 (dt, J 2.0, 8.0 Hz, 1H), 7.48-7.44 (m, 3H), 7.38 (t, J 8.0 Hz, 1H), 7.29-7.14 (m, 5H), 7.05-6.85 (m, 2H), 6.73 (ddd, J 1.0, 3.5, 8.0 Hz, 1H), 5.92 (s, 1H), 3.76 (s, 3H); ^{13}C NMR (100 MHz, CDCl₃): δ 167.4, 160.4, 156.1, 154.8, 141.9, 141.1, 130.5, 129.9, 129.2, 129.1, 129.0, 128.9, 128.8, 127.3, 127.0, 126.6, 119.3, 116.6, 114.6, 114.1, 52.8; IR (film): 3393, 1741, 1597, 1445, 1332, 1220, 783, 694 cm^{-1} ; LRMS (m/z , ES⁻): 370 ([M - 1]⁻, 80%); HRMS (m/z , ES⁺): [M + H]⁺ calcd. for C₂₃H₁₈NO₄, 372.1231; found, 372.1238.

Following the procedure outlined for the preparation of the carboxylic acid **1**, methyl 4-(3'-hydroxy-3-biphenyl)-5-phenylisoxazole-3-carboxylate (50 mg, 0.135 mmol) in MeOH (2 mL) and aqueous sodium hydroxide (2 M, 1.1 mL, 2.15 mmol), after recrystallisation (light petroleum:EtOAc, 100:1 v/v), gave the *title compound 7* as a white solid (40 mg, 0.11 mmol, 82%); mp: 189.9-190.8 °C; TLC (light petroleum:EtOAc, 50:50 v/v with 0.1% TFA): $R_f = 0.49$; HPLC (silica, EtOAc with 0.1 % TFA): retention time 3.22 min, 100 %; ^1H NMR (400 MHz, DMSO- d_6): δ 14.02 (br. s, 1H), 9.55 (s, 1H), 7.66 (ddd, J 1.5, 2.0, 8.0 Hz, 1H), 7.61 (dd, J 1.5, 2.0 Hz, 1H), 7.52-7.42 (m, 6H), 7.33 (dt, J 1.5, 7.5 Hz, 1H), 7.23 (t, J 8.0 Hz, 1H), 7.03 (d, J 8.0 Hz, 1H), 6.99 (t, J 2.0 Hz, 1H), 6.76 (dd, J 2.0, 8.0 Hz, 1H); ^{13}C NMR (100 MHz, DMSO- d_6): δ 171.8, 163.1, 157.8, 157.6, 157.8, 157.6, 140.9, 140.4, 130.7, 130.0, 129.8, 129.2, 129.1, 129.0, 128.2, 126.8, 126.6, 117.4, 114.7, 113.5; IR (film): 3066, 1736, 1598, 1489, 1458, 1429, 1349, 1322, 1240, 1210, 1023, 992, 896, 866, 810, 785, 764, 719 cm^{-1} ; LRMS (m/z , ES $^-$): 312 ([M - 45] $^-$, 100%); HRMS (m/z , ES $^-$): [M - CO $_2$ H] $^-$ calcd. for C $_{21}$ H $_{14}$ NO $_2$, 312.1030; found, 312.1017.

4-(3',5'-Dichoro-3-biphenyl)-5-phenylisoxazole-3-carboxylic acid (8)

Following the procedure outlined for the preparation of the methyl 4-biphenylisoxazole-3-carboxylate **22**, the aryl triflate **19** (290 mg, 0.68 mmol) and 3,5-dichlorophenylboronic acid (143 mg, 0.75 mmol) in DMF (7 mL) together with Pd(PPh $_3$) $_4$ (8 mg, 0.007 mmol), after repeated chromatography (Et $_2$ O:light petroleum, 20:80 - 40:60 v/v, then with DCM), gave methyl 4-(3',5'-dichoro-3-biphenyl)-5-phenylisoxazole-3-carboxylate as a white solid (120 mg, 0.28 mmol, 42%); TLC (Et $_2$ O:light petroleum, 40:60 v/v): $R_f = 0.51$; ^1H NMR (500 MHz,

CDCl₃): δ 7.52 (d, *J* 7.5 Hz, 1H), 7.45-7.42 (m, 4H), 7.34-7.30 (m, 4H), 7.27-7.23 (m, 3H), 3.82 (s, 3H); ¹³C NMR (125 MHz, CDCl₃): δ 167.4, 160.3, 154.7, 143.3, 138.9, 135.2, 130.5, 130.2, 129.7, 129.4, 128.9, 128.8, 127.4, 127.0, 126.6, 125.6, 116.1, 52.8; IR (film): 3074, 1740, 1585, 1560, 1444, 1334, 1220, 1175, 1100, 1028, 973, 857, 794, 770, 693 cm⁻¹.

Following the procedure outlined for the preparation of the carboxylic acid **1**, methyl 4-(3',5'-chloro-3-biphenyl)-5-phenylisoxazole-3-carboxylate (120 mg, 0.28 mmol) in MeOH (3 mL) and aqueous sodium hydroxide (2 M, 1 mL, 2.15 mmol), after recrystallisation (light petroleum:EtOA, 100:1 v/v), gave the *title compound* **8** as a white solid (55 mg, 0.13 mmol, 48%); mp: 169.9-171.0 °C; TLC (light petroleum:EtOAc, 50:50 v/v with 0.1% TFA): R_f = 0.53; HPLC (silica, EtOAc with 0.1 % TFA): retention time 4.29 min, 100 %; ¹H NMR (400 MHz, DMSO-*d*₆): δ 14.00 (br. s, 1H), 7.85-7.81 (m, 2H), 7.74 (d, *J* 2.0 Hz, 2H), 7.60 (m, 1H), 7.55-7.39 (m, 7H); ¹³C NMR (100 MHz, DMSO-*d*₆): δ 160.9, 156.1, 143.0, 139.3, 137.2, 134.7, 130.7, 129.8, 129.3, 129.1, 128.9, 127.1, 127.0, 126.9, 126.5, 125.5, 125.4, 115.9; IR (film): 3072, 1716, 1587, 1559, 1484, 1442, 1374, 1274, 1229, 1192, 1026, 987, 918, 856, 770, 720, 692 cm⁻¹.

4-(3',5'-Dimethyl-4'-hydroxy-3-biphenyl)-5-phenylisoxazole-3-carboxylic acid (9)

Following the procedure outlined for the preparation of the methyl 4-biphenylisoxazole-3-carboxylate **22**, the aryl triflate **19** (290 mg, 0.68 mmol) and 3,5-dimethyl-4-hydroxyphenylboronic acid (185 mg, 0.75 mmol) in DMF (7 mL) together with Pd(PPh₃)₄ (8 mg, 0.007 mmol), after repeated chromatography (Et₂O:light petroleum, 20:80 – 40:60 v/v, then with DCM), gave methyl 4-(3',5'-

dimethyl-4'-hydroxy-3-biphenyl)-5-phenylisoxazole-3-carboxylate as a white solid (154 mg, 0.39 mmol, 57%); TLC (Et₂O:light petroleum, 40:60 v/v): R_f = 0.20; ¹H NMR (500 MHz, CDCl₃): δ 7.69 (d, *J* 7.5 Hz, 1H), 7.66 (d, *J* 8.0 Hz, 2H), 7.60 (s, 1H), 7.55 (t, *J* 8.0 Hz, 1H), 7.48 (t, *J* 7.0 Hz, 1H), 7.43 (t, *J* 8.0 Hz, 2H), 7.36 (d, *J* 8.0 Hz, 1H), 7.27 (s, 2H), 4.87 (s, 1H), 3.98 (s, 3H), 2.37 (s, 6H); ¹³C NMR (125 MHz, CDCl₃): δ 167.3, 160.5, 155.0, 152.1, 141.5, 132.5, 130.4, 129.2, 129.0, 128.8, 128.5, 128.3, 127.4, 127.1, 126.9, 123.4, 116.8, 52.8, 16.1; IR (film): 3513, 2954, 1741, 1603, 1444, 1325, 1221, 1102, 1034, 974, 874, 816, 794, 769, 703 cm⁻¹.

Following the procedure outlined for the preparation of the carboxylic acid **1**, methyl 4-(3',5'-dimethyl-4'-hydroxy-3-biphenyl)-5-phenylisoxazole-3-carboxylate (150 mg, 0.38 mmol) in MeOH (4 mL) and aqueous sodium hydroxide (2 M, 1 mL, 2 mmol), after recrystallisation (light petroleum:EtOAc, 100:1 v/v), gave the *title compound* **9** as a white solid (79 mg, 0.20 mmol, 54%); mp: 182.3-182.9 °C; TLC (light petroleum:EtOAc, 50:50 v/v with 0.1% TFA): R_f = 0.55; HPLC (silica, EtOAc with 0.1 % TFA): retention time 3.80 min, 100 %; ¹H NMR (400 MHz, DMSO-*d*₆): δ 14.01 (br. s, 1H), 8.40 (s, 1H), 7.63 (d, *J* 8.0 Hz, 1H), 7.57 (s, 1H), 7.52-7.41 (m, 6H), 7.24 (d, *J* 7.5 Hz, 1H), 7.21 (s, 2H), 2.19 (s, 6H); ¹³C NMR (100 MHz, DMSO-*d*₆): δ 163.6, 161.1, 153.3, 140.6, 130.6, 130.3, 129.3, 129.1, 129.0, 127.8, 127.6, 126.8, 126.6, 126.0, 124.7, 124.5, 116.3, 113.2, 16.8; IR (film): 3474, 1713, 1601, 1490, 1433, 1315, 1227, 1204, 1178, 1031, 973, 928, 902, 868, 799, 773 cm⁻¹.

**4-(3'-Chloro-4'-hydroxy-3-biphenyl)-5-phenylisoxazole-3-carboxylic acid
(10)**

Following the procedure outlined for the preparation of the methyl 4-biphenylisoxazole-3-carboxylate **22**, the aryl triflate **19** (300 mg, 0.7 mmol) and 3-chloro-4-hydroxyphenylboronic acid (133 mg, 0.77 mmol) in DMF (7 mL) together with Pd(PPh₃)₄ (8 mg, 0.007 mmol), after repeated chromatography (Et₂O:light petroleum, 20:80 – 40:60 v/v then with DCM), gave methyl 4-(3'-chloro-4'-hydroxy-3-biphenyl)-5-phenylisoxazole-3-carboxylate as a white solid (180 mg, 0.44 mmol, 63%); mp: 60.3-61.9 °C; TLC (Et₂O:light petroleum, 40:60 v/v): R_f = 0.14; ¹H NMR (500 MHz, CDCl₃): δ 7.60-7.56 (m, 3H), 7.53-7.48 (m, 3H), 7.43-7.32 (m, 5H), 7.08 (d, *J* 8.5 Hz, 1H), 5.62 (s, 1H), 3.91 (s, 3H); ¹³C NMR (125 MHz, CDCl₃): δ 167.4, 160.5, 154.9, 151.0, 140.0, 134.2, 130.5, 129.5, 129.2, 129.1, 128.9, 128.6, 127.6, 127.2, 127.1, 126.9, 126.8, 120.3, 116.6, 116.5, 52.8; IR (film): 3419, 3061, 2955, 1740, 1608, 1508, 1485, 1464, 1444, 1387, 1335, 1287, 1221, 1177, 1102, 1054, 1021, 973, 909, 867, 816, 794, 770, 731, 706 cm⁻¹; LRMS (*m/z*, ES⁻): 406 ([M - 1]⁻, 65%), 404 ([M - 1]⁻, 100); HRMS (*m/z*, ES⁺): [M + H]⁺ calcd. for C₂₃H₁₇NO₄ ³⁵Cl, 406.0841; found, 406.0845.

Following the procedure outlined for the preparation of the carboxylic acid **1**, methyl 4-(3'-chloro-4'-hydroxy-3-biphenyl)-5-phenylisoxazole-3-carboxylate (157 mg, 0.39 mmol) in MeOH (4 mL) and aqueous sodium hydroxide (2 M, 1 mL, 2.15 mmol), after recrystallisation (light petroleum:EtOAc, 100:1 v/v), gave the *title compound* **10** as a white solid (80 mg, 0.2 mmol, 52% yield); mp: 171.8-175.0 °C; TLC (light petroleum:EtOAc, 50:50 v/v with 0.1% TFA): R_f = 0.5; HPLC (silica, EtOAc with 0.1 % TFA): retention time 3.20 min, 100 %; ¹H NMR (400 MHz, DMSO-*d*₆): δ 14.00 (br. s, 1H), 10.38 (s, 1H), 7.68-7.62 (m,

3H), 7.51-7.41 (m, 7H), 7.28 (d, *J* 7.5 Hz, 1H), 7.03 (d, *J* 8.5 Hz, 1H); ¹³C NMR (100 MHz, DMSO-*d*₆): δ 166.2, 161.0, 156.3, 152.9, 138.9, 131.5, 130.7, 129.5, 129.2, 129.1, 128.6, 127.9, 127.8, 126.9, 126.5, 126.3, 126.1, 120.3, 117.0, 116.1; IR (film): 3361, 1712, 1607, 1483, 1425, 1343, 1279, 1229, 1142, 1059, 930, 882, 866, 820, 802, 788, 771 cm⁻¹.

4-(3'-Fluoro-4'-hydroxy-3-biphenyl)-5-phenylisoxazole-3-carboxylic acid (11)

Following the procedure outlined for the preparation of the methyl 4-biphenylisoxazole-3-carboxylate **22**, the aryl triflate **19** (630 mg, 1.45 mmol) and 3-fluoro-4-hydroxyphenylboronic acid (250 mg, 1.6 mmol) in DMF (15 mL) with Pd(PPh₃)₄ (15 mg, 0.014 mmol), after repeated chromatography (Et₂O:light petroleum, 20:80 – 40:60 v/v, then with DCM) gave methyl 4-(3'-fluoro-4'-hydroxy-3-biphenyl)-5-phenylisoxazole-3-carboxylate as a white solid (260 mg, 0.67 mmol, 42%); mp: 63.4-65.0 °C; TLC (Et₂O:light petroleum, 30:70 v/v): R_f = 0.12; ¹H NMR (400 MHz, CDCl₃): δ 7.49-7.37 (m, 5H), 7.32-7.11 (m, 6H), 6.92 (t, *J* 8.5 Hz, 1H), 5.81 (s, 1H), 3.80 (s, 3H); ¹³C NMR (100 MHz, CDCl₃): δ 167.5, 160.6, 154.9, 152.5, 150.1, 143.3, 140.2, 133.5, 130.6, 129.4, 129.3, 129.0, 128.5, 127.1, 127.0, 126.8, 123.3, 117.7, 116.7, 114.4, 52.9; IR (film): 3363, 3059, 2955, 1737, 1621, 1522, 1444, 1215, 1104, 1021, 973, 868, 815, 789, 768, 749, 691 cm⁻¹.

Following the procedure outlined for the preparation of the carboxylic acid **1**, methyl 4-(3'-fluoro-4'-hydroxy-3-biphenyl)-5-phenylisoxazole-3-carboxylate (70 mg, 0.18 mmol) in MeOH (1.5 mL) and aqueous sodium hydroxide (2 M, 0.5 mL, 1.0 mmol), after recrystallisation (light petroleum:EtOAc, 100:1 v/v), gave the *title compound* **11** as a white solid (10 mg,

0.03 mmol, 17%); mp: 193.5-194.6 °C; TLC (light petroleum:EtOAc, 50:50 v/v with 0.1% TFA): R_f = 0.09; HPLC (silica, EtOAc with 0.1 % TFA): retention time 3.17 min, 100 %; $^1\text{H NMR}$ (500 MHz, $\text{DMSO-}d_6$): δ 13.99 (br. s, 1H), 10.03 (s, 1H), 7.69-7.66 (m, 2H), 7.52-7.42 (m, 7H), 7.31 (d, J 8.0 Hz, 1H), 7.28 (d, J 7.5 Hz, 1H), 7.00 (t, J 9.0 Hz, 1H); IR (film): 3261, 1719, 1621, 1522, 1443, 1216, 1118, 871, 796, 751, 691 cm^{-1} .

4-(3'-Chloro-4'-hydroxy-5'-nitro-3-biphenyl)-5-phenylisoxazole-3-carboxylic acid (12)

A mixture of 4-bromo-2-chloro-6-nitrophenol (1 g, 3.96 mmol), KOAc (1.17 g, 11.88 mmol), bis(pinacolato)diboron (1.21 g, 4.75 mmol) and [1,1'-bis(diphenylphosphino)ferrocene]palladium(II) dichloride (90 mg, 0.1188 mmol) in dioxane (40 mL) was stirred under nitrogen at 90 °C for 18 h before being poured into EtOAc (100 mL). The mixture was washed with aqueous hydrogen chloride (1 M, 100 mL), dried (MgSO_4) and concentrated under reduced pressure. Chromatography (Et_2O :light petroleum, 5:95 – 10:90 v/v) of the residue gave pinacolyl 3-chloro-4-hydroxy-5-nitrophenylboronate as a bright yellow solid (0.46 g, 1.54 mmol, 39%); TLC (Et_2O :light petroleum, 20:80, v/v): R_f = 0.69. The crude product was used in the next reaction.

Following the procedure outlined for the preparation of the methyl 4-biphenylisoxazole-3-carboxylate **22**, the aryl triflate **19** (295 mg, 0.69 mmol) and pinacolyl 3-chloro-4-hydroxy-5-nitrophenylboronate (310 mg, 1.04 mmol) in DMF (7 mL) with $\text{Pd}(\text{PPh}_3)_4$ (8 mg, 0.007 mmol), after repeated chromatography (Et_2O :light petroleum, 20:80 – 40:60 v/v then with DCM), gave methyl 4-(3'-chloro-4'-hydroxy-5'-nitro-3-biphenyl)-5-phenylisoxazole-3-carboxylate as a

white solid (45 mg, 0.103 mmol, 15%); mp: 74.5-75.7 °C; TLC (Et₂O:light petroleum, 30:70 v/v): R_f = 0.49; ¹H NMR (400 MHz, CDCl₃): δ 11.00 (s, 1H), 8.23 (d, *J* 2.5 Hz, 1H), 7.91 (d, *J* 2.5 Hz, 1H), 7.62 (m, 1H), 7.58-7.54 (m, 4H), 7.43 (d, *J* 7.5 Hz, 2H), 7.37 (d, *J* 7.5 Hz, 2H), 3.93 (s, 3H); ¹³C NMR (100 MHz, CDCl₃): δ 167.6, 160.4, 154.7, 150.7, 137.7, 136.2, 134.6, 132.8, 130.7, 130.4, 130.0, 129.7, 128.9, 128.7, 127.1, 126.9, 126.6, 125.1, 121.6, 116.1, 52.9; IR (film): 3223, 3078, 2948, 1737, 1621, 1539, 1218, 1173, 1110, 1029, 815, 692 cm⁻¹.

Following the procedure outlined for the preparation of the carboxylic acid **1**, methyl 4-(3'-chloro-4'-hydroxy-5'-nitrobiphenyl-3-yl)-5-phenylisoxazole-3-carboxylate (45 mg, 0.1 mmol) in MeOH (1 mL) and aqueous sodium hydroxide (2 M, 0.25 mL, 2 mmol), after recrystallisation (light petroleum:EtOAc, 100:1 v/v), gave the *title compound* **12** as a white solid (20 mg, 0.05 mmol, 46%); mp: 185.4-185.9 °C; TLC (light petroleum:EtOAc, 50:50 v/v with 0.1% TFA): R_f = 0.15; HPLC (silica, EtOAc with 0.1 % TFA): retention time 3.08 min, 100 %; ¹H NMR (500 MHz, DMSO-*d*₆): δ 13.97 (br. s, 1H), 11.30 (br. s, 1H), 8.16 (m, 1H), 8.14 (m, 1H), 7.84-7.80 (m, 2H), 7.54-7.41 (m, 6H), 7.37 (dd, *J* 1.0, 8.0 Hz, 1H); ¹³C NMR (125 MHz, DMSO-*d*₆): δ 166.3, 160.9, 156.2, 147.5, 138.6, 136.7, 133.1, 131.1, 130.6, 129.8, 129.7, 129.3, 129.1, 128.3, 126.8, 126.4, 124.6, 121.4, 116.0; IR (film): 3256, 3061, 2900, 1716, 1619, 1538, 1429, 1319, 1229, 1110, 906, 795, 763, 691 cm⁻¹.

4-(3',5'-Dichloro-4'-hydroxy-3-biphenyl)-5-methylisoxazole-3-carboxylic acid (13)

Trifluoromethanesulfonic anhydride (2.18 g, 7.72 mmol) was added to methyl 4-(3-hydroxyphenyl)-5-methylisoxazole-3-carboxylate (**25**) (1.2 g, 5.15 mmol) and

pyridine (1.01 g, 12.87 mmol) in dichloromethane (30 mL) at 0 °C and the reaction mixture was stirred at rt for 6 h then poured into water (30 mL). The mixture was extracted with dichloromethane (2 × 50 mL) and the organic extracts were dried (NaSO₄) and concentrated under reduced pressure. Chromatography of the residue (EtOAc:light petroleum, 20:80 v/v) gave the triflate **26** as an off-white solid (1.2 g, 66%); TLC (EtOAc:light petroleum, 10:90 v/v): R_f = 0.8; ¹H NMR (400 MHz, CDCl₃): δ 7.45 (m, 1H), 7.40-7.10 (m, 3H), 3.90 (s, 3H) 2.45 (s, 3H); LRMS (*m/z*, ES⁺): 306 ([M - 59]⁺, 100%).

Sodium carbonate in water (1.3 g, 12.3 mmol in 1 mL water) was added to a solution of methyl 5-methyl-4-(3-trifluoromethanesulfonyloxyphenyl)-isoxazole-3-carboxylate (**26**) (1.5 g, 4.10 mmol) and pinacolyl (3,5-dichloro-4-hydroxyphenyl)boronate (**21**) (1.77 g, 6.16 mmol) in DMF (10 mL) at 0 °C and the reaction mixture was degassed by bubbling nitrogen through for 15 min. The catalyst Pd(PPh₃)₄ (470 mg, 0.04 mmol) was added and the mixture heated to 90 °C for 3 h then cooled to rt and poured into ice-water (10 mL). The mixture was extracted with EtOAc (2 × 20 mL) and the organic extracts were dried (NaSO₄) and concentrated under reduced pressure to afford the methyl 4-(3',5'-dichloro-4'-hydroxy-3-biphenyl)-5-methylisoxazole-3-carboxylate (**27**) as an off-white solid (1.5 g) used without purification; TLC (EtOAc:light petroleum, 5:95 v/v): R_f = 0.5; LRMS (*m/z*, ES⁻) 376 ([M(Cl³⁵)₂ - 1]⁻, 100%), 378 ([M(Cl³⁵Cl³⁷) - 1]⁻, 65%), 380 ([M(Cl³⁷)₂ - 1]⁻, 10%).

Aqueous sodium hydroxide (152 mg in 1 mL water, 3.8 mmol) was added to the methyl ester **27** (500 mg, 1.19 mmol) in MeOH:THF (12 mL, 3:1 v/v) at 0 °C and the mixture stirred for 1 h at 0 °C then poured into ice-water (5 mL). The mixture was acidified to pH~1 using aqueous hydrochloric acid (2M) and

concentrated under reduced pressure to give aqueous slurry that was extracted with EtOAc (3 × 10 mL). The organic extracts were dried (NaSO₄) and concentrated under reduced pressure to give an off-white solid that was crystallized (light petroleum:EtOAc, 90:10 v/v) to give the *title compound 13* (315 mg, 65%) as an off-white solid; TLC (MeOH:dichloromethane, 10:90 v/v): R_f = 0.2; ¹H NMR (400 MHz, DMSO-*d*₆): δ 13.87 (br. s, 1H), 10.27 (s, 1H), 7.75-7.60 (m, 4H), 7.50 (t, *J* 7.6 Hz, 1H), 7.34 (d, *J* 7.6 Hz, 1H), 2.47 (s, 3H); ¹³C NMR (100 MHz, DMSO-*d*₆): δ 168.6, 162.0, 155.4, 149.1, 137.9, 133.1, 130.0, 129.4, 129.2, 128.1, 127.1, 126.3, 123.3, 116.5 and 11.8; LRMS (*m/z*, ES⁺) 364 ([M(Cl³⁵)₂ + 1]⁺, 100%), 366 ([M(Cl³⁵Cl³⁷) + 1]⁺, 50%), 368 ([M(Cl³⁷)₂ + 1]⁺, 10%).

Methyl 5-phenylisoxazole-3-carboxylate (14) ^{20 21}

Sodium methoxide (18.36 g, 340 mmol) in MeOH (80 mL) was added to acetophenone (20 mL, 161.92 mmol) and dimethyl oxalate (28.66 g, 242.9 mmol) in MeOH (450 mL) at rt and the solution was stirred at rt for 2 h before being cooled to rt and poured into aqueous hydrogen chloride (2 M, 800 mL). The solid methyl 2,4-dioxo-4-phenylbutanoate was filtered off, washed with water and used the next step without further purification.

Hydroxylamine hydrochloride (10.8 g, 154.6 mmol) was added to the methyl 2,4-dioxo-4-phenylbutanoate (21.37 g, 103 mmol) in MeOH (520 mL) and the mixture was stirred under reflux for 24 hours. After cooling to rt, the mixture was poured into water (1 L) and cooled to 0 °C. The white precipitate was filtered off, washed with water, and then dissolved in EtOAc. The solution was dried (MgSO₄) and concentrated under reduced pressure to give the *title compound 14* as a white solid (18.4 g, 90.6 mmol, 88%); mp: 81.8 – 82.5 °C (lit. ²¹

80-82 °C); TLC (Et₂O:light petroleum, 10:90 v/v): R_f = 0.2; ¹H NMR (300 MHz, DMSO-*d*₆): δ 7.98-7.92 (m, 2H), 7.57-7.52 (m, 3H), 7.51 (s, 1H), 3.92 (s, 3H); ¹³C NMR (75 MHz, DMSO-*d*₆): δ 171.1, 159.8, 156.6, 131.0, 129.3, 126.0, 125.8, 100.8, 52.8; IR (film): 3130, 2951, 1724, 1612, 1591, 1571, 1445, 1425, 1246, 1141, 1004, 946, 934, 920, 851, 837, 807, 781, 764 cm⁻¹.

Methyl 4-bromo-5-phenylisoxazole-3-carboxylate (15) ²²

N-Bromosuccinimide (6.85 g, 38.47 mmol) was added to methyl 5-phenylisoxazole-3-carboxylate **14** (7.1 g, 34.98 mmol) in trifluoroacetic acid (100 mL) and solution stirred under reflux for 48 h before being cooled to rt and poured onto ice. The white precipitate was filtered off and recrystallised (light petroleum:EtOAc, 100:1 v/v) to give the title compound **15** as white crystals (6.35 g, 22.5 mmol, 64%); mp: 108-110 °C (lit. ²² 66-68 °C); TLC (Et₂O:light petroleum, 10:90 v/v): R_f = 0.23; ¹H NMR (400 MHz, DMSO-*d*₆): δ 8.02-7.98 (m, 2H), 7.65-7.60 (m, 3H), 3.94 (s, 3H); ¹³C NMR (100 MHz, DMSO-*d*₆): δ 167.2, 158.9, 154.6, 131.8, 129.5, 127.1, 125.4, 90.1, 53.3; IR (film): 1732, 1565, 1436, 1414, 1252, 1215, 1183, 1046, 970, 810, 785, 771 cm⁻¹; LRMS (ES⁺, *m/z*): 306 ([M + 23]⁺, 100%), 304 ([M + 23]⁺, 90%); HRMS (*m/z*): [M + H]⁺ calcd. for C₁₁H₉NO₃⁷⁹Br, 281.9761; found, 281.9759.

Methyl 4,5-diphenylisoxazole-3-carboxylate (16) ²³

A solution of methyl 4-bromo-5-phenylisoxazole-3-carboxylate **15** (100 mg, 0.35 mmol) and phenylboronic acid (52 mg, 0.42 mmol) in DMF (4 mL) was degassed by bubbling nitrogen through it for 30 min. Aqueous sodium carbonate (2 M, 0.5

mL, 1.0 mmol) was added and nitrogen was bubbled through the mixture for a further 15 min. Bis(triphenylphosphine)palladium(II) dichloride (12 mg, 0.02 mmol) was added and the mixture stirred at 90 °C for 3 hours. The mixture was cooled to rt and poured into EtOAc (20 mL). The mixture was washed with aqueous hydrogen chloride (2 M, 20 mL), water (20 mL) and brine (20 mL), then dried (NaSO₄) and concentrated under reduced pressure. Chromatography (Et₂O:light petroleum, 20:80 – 40:60 v/v) of the residue gave the title compound **16** as an off-white solid (94 mg, 0.34 mmol, 80%); TLC (Et₂O:light petroleum, 20:80 v/v): R_f = 0.40; ¹H NMR (400 MHz, DMSO-*d*₆): δ 7.55-7.41 (m, 10H), 3.84 (s, 3H); ¹³C NMR (100 MHz, DMSO-*d*₆): δ 166.6, 159.9, 155.0, 130.8, 130.1, 129.1, 128.7, 128.6, 128.5, 126.8, 126.3, 116.5, 52.8; LRMS (ES⁺, *m/z*): 302 ([M + 23]⁺, 100%), 280 ([M + 1]⁺, 10); HRMS (*m/z*): [M + H]⁺ calcd. for C₁₇H₁₄NO₃, 280.0969; found, 280.0970.

Methyl 4-(3-methoxyphenyl)-5-phenylisoxazole-3-carboxylate (17)

A solution of methyl 4-bromo-5-phenylisoxazole-3-carboxylate **15** (6.68 g, 23.7 mmol) and 3-methoxyphenylboronic acid (4.3 g, 28.4 mmol) in DMF (230 mL) was degassed by bubbling nitrogen through it for 30 min. Aqueous sodium carbonate (2 M, 36 mL, 72 mmol) was added and nitrogen was bubbled through the mixture for a further 15 min. The catalyst Pd(PPh₃)₄ (300 mg, 0.24 mmol) was added and the mixture was stirred at 90 °C for 3 hours. The mixture was cooled to rt and poured into EtOAc (250 mL). The resulting mixture was washed with aqueous hydrogen chloride (2 M, 250 mL), water (250 mL) and brine (250 mL) then dried (NaSO₄) and concentrated under reduced pressure. Chromatography (Et₂O:light petroleum, 20:80 – 40:60 v/v) of the residue gave

the *title compound 17* as a pale yellow solid (3.1 g, 9.95 mmol, 42%); mp: 110.5-111.9 °C; TLC (Et₂O:light petroleum, 40:60, v/v): R_f = 0.37; ¹H NMR (500 MHz, CDCl₃): δ 7.46 (d, *J* = 7.0 Hz, 2H), 7.32-7.24 (m, 4H), 6.90 (dd, *J* 2.5, 8.0 Hz, 1H), 6.85 (d, *J* 7.5 Hz, 1H), 6.81 (m, 1H), 3.81 (s, 3H), 3.71 (s, 3H); ¹³C NMR (125 MHz, CDCl₃): δ 167.2, 160.4, 159.7, 155.0, 130.4, 130.2, 129.8, 128.8, 127.0, 126.8, 122.5, 116.6, 115.8, 114.2, 55.3, 52.8; IR (film): 3012, 2956, 2843, 1736, 1587, 1420, 1331, 1243, 1213, 1164, 1094, 1043, 971, 872, 843, 789, 768, 709, 691 cm⁻¹; LRMS (ES⁺, *m/z*): 332 ([M + 23]⁺, 100%); HRMS (*m/z*): [M + H]⁺ calcd. for C₁₈H₁₆NO₄, 310.1074; found, 310.1071.

Methyl 4-(3-hydroxyphenyl)-5-phenylisoxazole-3-carboxylate (18)

A solution of methyl 4-bromo-5-phenylisoxazole-3-carboxylate **15** (9.3 g, 32.95 mmol) and 3-hydroxyphenylboronic acid (5 g, 36.5 mmol) in DMF (330 mL) was degassed by bubbling nitrogen through it for 1 hour. Aqueous sodium carbonate (2 M, 49.4 mL, 98.85 mmol) was added and nitrogen was bubbled through the mixture for a further 15 min. The catalyst Pd(PPh₃)₄ (380 mg, 0.33 mmol) was added and the mixture stirred at 90 °C for 90 min. The mixture was cooled to rt and poured into EtOAc (1 L). The mixture was washed with aqueous hydrogen chloride (2 M, 500 mL), water (1 L) and brine (1 L) then dried (NaSO₄) and concentrated under reduced pressure. Repeated chromatography of the residue (Et₂O:light petroleum, 20:80 – 40:60 v/v, then DCM) gave the *title compound 18* as an off-white solid (4.76 g, 16.1 mmol, 49%); mp: 148.7-149.9 °C; TLC (Et₂O:light petroleum, 40:60 v/v): R_f = 0.24; ¹H NMR (400 MHz, MeOD): δ 7.48-7.45 (m, 2H), 7.38-7.28 (m, 3H), 7.19 (t, *J* 8.0 Hz, 1H), 6.82 (ddd, *J* 1.0, 2.5, 8.5 Hz,

1H), 6.72-6.70 (m, 2H), 4.65 (s, 1H), 3.77 (s, 3H); ¹³C NMR (100 MHz, MeOD): δ 168.4, 161.8, 158.9, 156.6, 131.7, 131.5, 131.2, 131.0, 130.0, 128.2, 128.1, 122.4, 118.1, 116.7, 53.2; IR (film): 3473, 1745, 1590, 1449, 1331, 1216, 1164, 1094, 1035, 985, 865, 811, 788, 774, 706, 691 cm⁻¹; LRMS (*m/z*, ES⁺): 318 ([M + 23]⁺, 100%); HRMS (*m/z*): [M + H]⁺, calc. for C₁₇H₁₄NO₄, 296.0918; found, 296.0913.

Methyl 5-phenyl-4-(3-trifluoromethylsulfonyloxyphenyl)isoxazole-3-carboxylate (19)

Trifluoromethanesulphonic anhydride (1 M in DCM, 16.27 mL, 16.27 mmol) was added to methyl 4-(3-hydroxyphenyl)-5-phenylisoxazole-3-carboxylate **18** (4 g, 13.56 mmol) and pyridine (2.18 mL, 27.12 mmol) in DCM (135 mL) at 0 °C and the reaction mixture was stirred at rt for 90 min before being poured into EtOAc (800 mL). The solution was washed with aqueous hydrogen chloride (1 M, 800 mL), dried (MgSO₄) and concentrated under reduced pressure. Chromatography (Et₂O:light petroleum, 20:80 v/v) of the residue gave the *title compound 19* as a white solid (5.47 g, 12.75 mmol, 94%); mp: 95.0 – 96.7 °C; TLC (Et₂O:light petroleum, 40:60 v/v): R_f = 0.41; ¹H NMR (400 MHz, CDCl₃): δ 7.55 (t, *J* 8.0 Hz, 1H), 7.49-7.35 (m, 7H), 7.31 (dd, *J* 1.5, 2.0 Hz, 1H), 3.91 (s, 3H); ¹³C NMR (100 MHz, CDCl₃): δ 239.2, 168.0, 160.2, 154.6, 149.5, 131.7, 131.0, 130.6, 129.1, 127.1, 126.2, 123.5, 121.6, 114.6, 53.0; IR (film): 3068, 2968, 1738, 1418, 1248, 1210, 1128, 971, 917, 897, 815, 771, 686 cm⁻¹; LRMS (*m/z*, ES⁺): 450 ([M + 23]⁺, 45%).

Pinacolyl (3,5-dichloro-4-hydroxyphenyl)boronate (21)

A mixture of 4-bromo-2,6-dichlorophenol **20** (7 g, 28.94 mmol), KOAc (8.52 g, 86.8 mmol), bis(pinacolato)diboron (8.82 g, 34.73 mmol) and [1,1'-bis(diphenylphosphino)ferrocene]palladium(II) dichloride (640 mg, 0.87 mmol) in dioxane (300 mL) was stirred under nitrogen at 90 °C for 18 h before being poured into EtOAc (600 mL). The mixture was washed with aqueous hydrogen chloride (1 M, 600 mL), dried (MgSO₄) and concentrated under reduced pressure. Chromatography (Et₂O:light petroleum, 10:90 v/v) of the residue gave the *title compound* **21** as a pale yellow solid (4.9 g, 16.96 mmol, 59%); mp: 103.3-104.2 °C; TLC (Et₂O:light petroleum, 10:90 v/v): R_f = 0.38; ¹H NMR (400 MHz, CDCl₃): δ 7.61 (s, 2H), 5.99 (s, 1H), 1.26 (s, 12H); ¹³C NMR (100 MHz, CDCl₃): δ 150.0, 134.5, 128.3, 120.9, 84.3, 24.8; IR (film): 3271, 2980, 1592, 1384, 1349, 1230, 1129, 961, 892, 848, 788, 676 cm⁻¹; LRMS (*m/z*, ES⁻): 287 ([M - 1]⁻, 100%); HRMS (*m/z*, ES⁻): [M - H]⁻ calcd. for C₁₂H₁₄O₃³⁵Cl₂B, 287.0418; found, 287.0405.

Methyl 4-(3',5'-dichloro-4'-hydroxy-3-biphenyl)-5-phenylisoxazole-3-carboxylate (22); standard procedure

A solution of methyl 5-phenyl-4-(3-trifluoromethylsulfonyloxyphenyl)isoxazole-3-carboxylate **19** (1.9 g, 4.47 mmol) and the boronate **21** (1.42 g, 4.91 mmol) in DMF (50 mL) was degassed by bubbling nitrogen through it for 30 min. Aqueous sodium carbonate (2 M, 6.7 mL, 13.41 mmol) was added and nitrogen was bubbled through the solution for a further 15 min. The catalyst Pd(PPh₃)₄ (50 mg, 0.045 mmol) was added and the mixture stirred at 90 °C for 3 h then cooled to rt and poured into EtOAc (100 mL). The mixture was washed with aqueous hydrogen chloride (2 M, 100 mL), water (100 mL) and brine (100 mL), then

dried (NaSO₄) and concentrated under reduced pressure. Chromatography (Et₂O:light petroleum, 20:80 – 40:60 v/v) of the residue gave an off white solid that was recrystallised (light petroleum:EtOAc, 70:30 v/v) to give the *title compound 22* as a white solid (900 mg, 2.05 mmol, 45%); mp: 149.7-150.5 °C; TLC (Et₂O:light petroleum, 40:60 v/v): R_f = 0.26; ¹H NMR (400 MHz, CDCl₃): δ 7.59-7.49 (m, 5H), 7.46 (s, 2H), 7.43-7.34 (m, 4H), 5.91 (s, 1H), 3.92 (s, 3H); ¹³C NMR (100 MHz, CDCl₃): δ 167.5, 160.4, 154.8, 147.3, 138.8, 134.2, 130.6, 129.7, 129.6, 129.4, 128.9, 128.6, 127.1, 126.9, 126.7, 121.5, 116.3, 104.8, 52.8; IR (film): 3404, 1719, 1500, 1465, 1438, 1340, 1296, 1228, 1156, 1030, 973, 866, 820, 790, 765, 688 cm⁻¹; LRMS (*m/z*, ES⁻): 442 ([M - 1]⁻, 20%), 440 ([M - 1]⁻, 50), 438 ([M - 1]⁻, 100); HRMS (*m/z*, ES⁻): [M - H]⁻ calcd. for C₂₃H₁₄NO₄³⁵Cl₂, 438.0305; found, 438.0299.

Methyl 4-(3-hydroxyphenyl)-5-methylisoxazole-3-carboxylate (25)

Hydroxylamine hydrochloride (1.44 g, 20.8 mmol) was added to methyl 2,4-dioxopentanoate (2 g, 13.89 mmol) in MeOH (50 mL) and the reaction mixture stirred under reflux for 16 hours. After cooling to rt the mixture was poured into water (50 mL) and the solution extracted with EtOAc (2 × 50 mL). The extracts were dried (Na₂SO₄) and concentrated under reduced pressure to afford the methyl 5-methylisoxazole-3-carboxylate (**23**)³² (1.1 g) used without purification; TLC (EtOAc:light petroleum, 20:80 v/v): R_f = 0.50; ¹H NMR (400 MHz, CDCl₃): δ 6.41 (s, 1H) 3.96 (s, 3H) 2.50 (s, 3H); LRMS (*m/z*, ES⁺): 142 ([M + 1]⁺, 100%).

N-Bromosuccinimide (965 mg, 8.578 mmol) was added to methyl 5-methyl-isoxazole-3-carboxylate (**23**) (1.1 g, 7.799 mmol) in trifluoroacetic acid

(15 mL) at 0 °C and the solution heated under reflux for 16 hours, then allowed to cool to rt and poured onto ice-water (20 mL). The mixture extracted with EtOAc (2 × 50 mL), and the organic extracts were dried (Na₂SO₄) then concentrated under reduced pressure to afford methyl 4-bromo-5-methylisoxazole-3-carboxylate (**24**)³³ (1.2 g) as a white solid used without purification; TLC (EtOAc:light petroleum, 20:80 v/v): R_f = 0.40; ¹H NMR (400 MHz, CDCl₃): δ 3.89 (s, 3H) 2.50 (s, 3H); LRMS (*m/z*, ES⁺): 221 ([M + 1]⁺, 100%).

Aqueous sodium hydrogen carbonate (575 mg, 6.89 mmol in 1 mL water) was added to methyl 4-bromo-5-methylisoxazole-3-carboxylate (**24**) (500 mg, 2.28 mmol) and 3-hydroxyphenylboronic acid (346 mg, 2.51 mmol) in DMF (5 mL) at 0 °C and the reaction mixture was degassed for 30 min with argon. The catalyst Pd(PPh₃)₂Cl₂ (160 mg) was added rt and the mixture heated at 90 °C for 5 h then cooled to rt and poured onto ice-water (20 mL). The mixture was extracted with EtOAc (2 × 50 mL) and the organic extracts were dried (Na₂SO₄) and concentrated under reduced pressure. Chromatography of the residue (EtOAc:light petroleum, 20:80 v/v) gave the *title compound* **25** as an off-white solid (150 mg, 28%); TLC (EtOAc:light petroleum, 30:70 v/v): R_f = 0.3; ¹H NMR (400 MHz, CDCl₃): δ 7.30 (m, 1H) 6.90-6.75 (m, 3H) 4.83 (s, 1H), 3.90 (s, 3H), 2.45 (s, 3H).

Recombinant protein production

The Rv2234 and Rv0153c genes, encoding MptpA and MptpB, were amplified from *M. tuberculosis* H37Rv and cloned into vector pET28a as previously described¹¹. Site-directed mutagenesis was performed on wild-type pET28-MptpB, using QuikChange® (Stratagene), to generate the mutants H94A, Y125A,

E129A and R136A. His-tagged MptpA, MptpB and derivatives thereof were expressed in *Escherichia coli* BL21(DE3), with expression induced at 18°C with 0.5 mM IPTG for 16 hours, and purified by sequential nickel-affinity (in 50 mM HEPES, 500 mM NaCl, pH 7 buffer) and anion-exchange chromatography using MonoQ column (GE Healthcare) in 20 mM Tris, pH 8 and eluted in a NaCl gradient. Fractions were concentrated and further purified on a Superdex75 column (Amersham Bioscience) with 20 mM Tris, 300 mM NaCl pH 8. The VHR construct, in pGEX-4T, was a gift from Prof. Rafael Pulido (BioCruces Health Research Institute, Barakaldo, Spain) and the hPTP1B in pGEX-KG a gift from Prof. Jeroen der Hertog (Hubrecht Institute, Utrecht, Netherlands). The plasmids were transformed into *E. coli* and protein expression induced at 18°C with 0.5 mM IPTG for 16 hours. Purification of glutathione S-transferase (GST)-tagged proteins was achieved by GST affinity chromatography in 50 mM HEPES, 500 mM NaCl, pH 7 buffer and eluted with 20 mM glutathione. GST tag was removed by protease cleavage and subsequently purified using a Superdex 75 column in 50 mM HEPES buffer at pH 7.

Inhibition assays

Inhibition assays were performed as previously described¹³, where each titration experiment was performed in triplicate, and in at least three independent assays. Experiments were conducted in 96-well microtiter plates and each well contained a 100 μ L reaction mixture including 0.5 μ g of protein, in 50 mM Tris, 50 mM BisTris, 100 mM sodium acetate buffer (pH 7 for MptpB, pH 6.5 for MptpA, pH 6 for hPTP1B and pH 5 for VHR), and the different compounds dissolved in DMSO at a concentration range between 0-250 μ M. Reactions were

incubated for 15 min at room temperature before the addition of *p*-nitro phenyl phosphate (pNPP) to a final concentration of 0.35 mM. After 15 min incubation, the reactions were quenched by the addition of 0.5 M NaOH and the absorbance at 405 nm was measured. Production of *p*-nitro phenol (pNP) was quantified using a pNP (Sigma) calibration curve (2–2000 μ M). Control reactions without enzyme were performed to account for the spontaneous hydrolysis of pNPP. Phosphate release was calculated as a percentage of the specific activity and plotted as a function of inhibitor concentration to determine the IC₅₀.

Computational virtual screening and molecular docking

The computational fragment screening was done using the massive processing algorithm (MPA), a high throughput virtual screening genetic based algorithm^{18, 19} that combines ligand docking to the target using Autodock4³⁴, with text based (LINGO) similarity searches of the compound library³⁵. The MPA algorithm was used to search nine different commercial libraries that contained either building blocks (for rapid synthesis approaches) or fragments from different sources. The crystal structure of MptpB (PDB ID: 2OZ5) was used in the screening and a grid box was defined around the secondary P2 pocket. Compounds were scored according to their calculated binding energy (ΔG) and their mode of binding analysed graphically using PyMol (Schrödinger). Synthesized compounds were docked to the crystal structure of MptpB (PDB ID: 2OZ5), using AutoDock4³⁴. All compounds were docked using the default parameters and a maximum of 10 conformations were generated per ligand. Each docking conformation was scored according to their calculated free energy of binding, ΔG .

Bacterial strains, cell culture and infections

Mycobacterium tuberculosis strain H37Rv (ATCC35837, drug susceptible), the clinical isolate "W_565"³⁶ of multidrug-resistant *M. tuberculosis*, and *Mycobacterium bovis* Bacille Calmette-Guerin (BCG, Pasteur) were grown at 37°C in Middlebrook 7H9 broth containing 0.05% Tween 80 with shaking or on Middlebrook 7H10 agar (both types of medium were supplemented with 10% oleic acid/albumin/dextrose/catalase enrichment and 0.5% glycerol).

For infections using BCG, J774A.1 macrophages (ATCC) were cultured in Dulbecco's modified Eagle's medium (Sigma) containing glucose (25 mM) and L-glutamine (4 mM) supplemented with 10% heat inactivated fetal bovine serum (FBS, Invitrogen) at 37°C in a humidified atmosphere with 5% CO₂. For infections, J774A.1 cells were seeded in 96-well culture plates (Corning) at a density of 2×10^3 per well (in 200 µl of media) and incubated overnight. Cells were subsequently washed twice in pre-warmed Dulbecco's PBS (Sigma) and 100 µl of fresh culture medium, supplemented with inhibitors (dissolved in dimethyl sulphoxide, DMSO) or DMSO alone, added before infecting with BCG in 100 µl of medium at a multiplicity of infection (MOI) of 10:1 (bacteria:macrophage). After 4 h of infection, cells were washed four times with Dulbecco's PBS to remove extracellular bacteria and 200 µl of fresh culture medium (supplemented with inhibitors or DMSO) added; this was defined as time 0 hours. At 24 hours post infection, the cells were again washed twice with Dulbecco's PBS and fresh medium (supplemented with inhibitors or DMSO) added. At 72 hours post infection, infected cells were lysed in 0.05% (v/v) Tween 80 and the number of viable bacteria in each well determined by plating 10-fold serial dilutions on Middlebrook 7H10 agar plates in triplicates. The

plates were incubated for 3 weeks at 37 °C prior to counting the number of viable bacteria. All assays were performed in triplicate in at least three separate experiments.

For infections using *M. tuberculosis*, bacteria were grown for 1 week at 37°C with shaking and then washed with PBS and frozen (in 7H9 with 15% of Glycerol) at a concentration of 4×10^7 CFU ml⁻¹. THP1 macrophage cells were sub-cultured in RPMI 1640 (Gibco), supplemented with 10% FBS and 4 mM L-glutamine and then 1×10^6 cells were aliquoted per well (6-well plates) and treated with PMA overnight. The media was removed the following day and the cells were washed with PBS, and 1.5 ml of fresh RPMI (with 10% FBS) and inhibitors (0, 20 or 80 µM in DMSO) was added, before infecting with thawed *M.tuberculosis* at MOI of 1:1. After 3 hours of infection, THP1 cells were washed 4 times with PBS, and fresh RPMI was added. After 24 hours the media was removed and cells were washed with PBS prior to the addition of fresh RPMI and inhibitor (20 or 80 µM, dissolved in DMSO). At 72 hours post infection, cells were washed with PBS, lysed with 0.05% SDS and plated onto 7H10 media to determine bacterial numbers. Plates were counted after 3 weeks of growth at 37 °C (all experimental points were plated as 10-fold serial dilutions in duplicates). Each experiment was done in triplicate, including controls.

Cytotoxicity assays

Macrophage viability was measured using the (3-(4,5-Dimethylthiazol-2-yl)-2,5-Diphenyltetrazolium Bromide) (MTT) assay³⁷. Briefly, J774A.1 cells were seeded in 96-well culture plates (Corning) at a density of 6×10^3 (200µl/well) and allowed to adhere overnight. Fresh media supplemented with inhibitors

(dissolved in dimethyl sulphoxide, DMSO) or DMSO only were subsequently added to each well. Cell viability at 24 hours was assessed by adding 50 μ l of filter sterilised MTT (5 mg ml⁻¹ in PBS) to each well followed by a 4 hour incubation. Media was removed and 200 μ l of DMSO and 25 μ l of Sorensen's glycine buffer were added. The absorbance at 570 nm was measured in a plate reader.

Live cell imaging of *M. tuberculosis*-infected macrophages

RAW264.7 macrophages were grown in complete DMEM + 10 % FBS. On the day before infection with RFP, *M. tuberculosis* (4x 10⁵ cells) were plated on WillCo glass bottom dishes (22mm, GWST-3522). Cells were left for approximately 6 hours at 37 °C to attach before transfection using JetPEI-macrophage (polyplus) transfection reagents. EGFP-2xFYVE plasmid, 1.5 μ g, and 4 μ l JetPEI transfection reagent in 100 μ l of 150 mM NaCl were used for transfection of one dish.

The day after transfection a single cell suspension of RFP-Mtb H37Rv was prepared and added to the dish at MOI 5:1 together with the lead compound **13** (80 μ M). Directly after addition of bacteria the cells were imaged. Images were taken every 30 seconds at 512x512 resolution, z=3, 3x line average ²⁴.

Pharmacokinetic evaluations

Guinea pig males (Durkin Hartley) were used to evaluate the pharmacokinetics and tissue distribution of compounds. The route of administration was either intraperitoneal (IP) or oral (PO) with dosage varying from 3.5-8 mgkg⁻¹ (OP) and 2.5-4 mg kg⁻¹ (IP). In each case 4 samples were collected per time-point at 0.1, 0.5, 2, 4 and 8 h post dose for IP and 0.25, 0.5, 2, 4 and 8 h post dose for PO.

Compounds were prepared in 10% DMSO, 5% Cremaphor, 85% physiological saline for IP administration, or 0.5% (v/v) Tween 80, 99.5% (v/v) 0.5% Methylcellulose for oral administration. Tissue samples (n=4) from lung, liver and kidney were collected at the end of the study and snap frozen prior to bioanalysis.

Efficacy studies in guinea pigs

All animals were housed in the Public Health Research Institute's Animal Biosafety Level-2 (tolerability) or Animal Biosafety Level-3 (efficacy) Research Animal Facility (ICPH RAF), a center of the New Jersey Medical School, Rutgers University (NJMS-Rutgers). The animal facility follows the Public Health Service and National Institute of Health Policy of Humane Care and Use of Laboratory Animals. All experimental protocols were approved by the Rutgers Institutional Animal Care and Use Committee (IACUC). Female outbred Hartley Duncan Guinea Pigs (~400 g) were used in all studies. Tolerability studies were done prior to the infection models. Guinea pigs (n=5) were orally dosed once daily for 7 days with **13** 50, or 100 mg kg⁻¹. No adverse drug effects were observed and weight increases of >5% was observed in all animals during the tolerability trial. Plasma and lung drug levels were analyzed at 2 and 24 hours (peak and trough levels) after the last dose administered. Drug levels for the 100 mg kg⁻¹ orally administered **13** were 1748 ng ml⁻¹ in plasma and 623 ng ml⁻¹ in lungs at 2 hours, and 35 ng ml⁻¹ in plasma at 24 hours.

An acute model of TB infection was used to assess the efficacy of compound **13**

as monotherapy in reducing bacterial burden during early acute phase of growth in the lungs. In this infection model, guinea-pigs were infected with 96 CFU (Average, \pm 27 SEM) of *M. tuberculosis* H37Rv via aerosol inhalation. The animals were randomized into groups of 4 Guinea pigs per treatment or vehicle group. The infection was confirmed by lung bacterial burden enumeration from 3 animals sacrificed at 24 hours post exposure. Compound **13** (100 mg kg⁻¹) and the vehicle were orally administered (feeding) daily for 4 weeks starting at 24 hours post infection. After 4 weeks of treatment, all guinea-pigs on the study gained weight and had normal behavior and fecal output.

A chronic model of TB infection was used to assess the efficacy of compound **13** as monotherapy (100 mg kg⁻¹). No morbidity was observed throughout the study. Guinea-pigs were infected with low dose *M. tuberculosis* with 63 CFU (Average, \pm 18 SEM) by aerosol inhalation. The animals were randomized into groups of 5 guinea pigs per treatment or vehicle group. The infection was confirmed by lung bacterial burden enumeration from 3 animals sacrificed at 24 hours post exposure. The remaining animals were left untreated for 4 weeks to develop a steady state of TB burdens in the lungs. After 28 days of infection, 4 animals were sacrificed and bacterial burdens of the lungs and spleens were enumerated to establish a baseline burden level prior to the start of treatment. Compound **13** (100 mg kg⁻¹) and the vehicle were orally administered daily for 4 weeks starting at 28 days post infection. After 4 weeks of treatment, all guinea pigs on the study did have varying increases in weight, and exhibited normal behavior and fecal output. For statistical analysis, the CFUs are converted to logarithms, and evaluated by a one-way ANOVA followed by a multiple comparison analysis of variance by Tukey and/or Dunnett's test (Graphpad

Prism 6.0 software program). Differences were considered significant at the 95% level of confidence. For both the acute and chronic infection studies, the lungs and spleens were graded from 1-4 based on a modified Mitchison virulence scoring from Jain et al.²⁷. The scoring was based on gross pathological examination of inflammation, extent of involvement and necrosis, number and relative size of lesions.

Histopathology

For histology, portions of guinea-pig lungs and spleens were fixed in neutral buffered formalin then embedded in paraffin. Sections, (~5 µm), were cut and stained with hematoxylin and eosin.

Author contributions

C.F.V., A.S., A.C., P.F., N.K., C.S. Y.N., generated compounds, tested their activity in vitro and in macrophage infections, supported computational screening, L.S.S. performed live imaging experiments and S.P. the animal studies. M.P., M.G.G, B.N.K., D.S.P., E.J.T. J.S.C. and L.T. supervised the work and analysed data. J.S.C. and L.T. wrote the paper, L.T. conceived and managed the project from the beginning.

Acknowledgements

This work was supported by funding from: MRC (G0701233) to L.T., E.J.T. and J.C., a MRC confidence in concept award, a BBSRC spark impact award, and a

Manchester Chemical Biology Network award to L.T. This work was partially supported by NIH U19AI109713 to D.S.P., MINECO BIO2016-78006-R to M.P., Catalan Government 2009PIV 00100 grants to L.T. and M.P., and the Francis Crick Institute to M.G.G., which receives its core funding from Cancer Research UK (FC001092), the UK Medical Research Council (MC_UP_1202/11, FC001092), and the Wellcome Trust (FC001092). We thank Peter Warn and Lloyd Pane at Euprotec/Evotec for advice and PK/PD analysis; William Hope (Liverpool University) and Redx Pharma ltd for initial evaluation of compounds and DMPK analysis, and LifeArc for evaluation of compound 13 and support to the project; Cele Abad-Zapatero, Scott Franzblau and Larry Klein (Univ. of Illinois in Chicago) for advice and useful discussions; Nicola Beresford for her early work in the project; Alexander Bruce and James Adams for support with inhibition experiments; Trevor Perrior (Domainex) and John Dixon for advice on medicinal chemistry; John Horton and Chris Reilly for advice, and David Denning for constant support, advice and encouragement

Competing financial interests

The authors declare no conflict of interests

Supporting Information

Suppl. Table 1, 2, 3, 4.

Suppl. Figure 1, 2, 3.

Spectra for compounds synthesised

Molecular Formula Strings are available online (Vickers-MFS.csv)

Additional Information

Correspondence and requests for materials should be addressed to L.T. :

Lydia.Tabernero@manchester.ac.uk

References

- 1 Armstrong, J. A. & Hart, P. D. Response of cultured macrophages to *Mycobacterium tuberculosis*, with observations on fusion of lysosomes with phagosomes. *J Exp Med* **134**, 713-740 (1971).
- 2 Rohde, K., Yates, R. M., Purdy, G. E. & Russell, D. G. *Mycobacterium tuberculosis* and the environment within the phagosome. *Immunol Rev* **219**, 37-54, doi:10.1111/j.1600-065X.2007.00547.x (2007).
- 3 Rasko, D. A. & Sperandio, V. Anti-virulence strategies to combat bacteria-mediated disease. *Nat Rev Drug Discov* **9**, 117-128, doi:10.1038/nrd3013 (2010).
- 4 Silva, A. P. & Taberner, L. New strategies in fighting TB: targeting *Mycobacterium tuberculosis*-secreted phosphatases MptpA & MptpB. *Future Med Chem* **2**, 1325-1337, doi:10.4155/fmc.10.214 (2010).
- 5 Cole, S. T. Inhibiting *Mycobacterium tuberculosis* within and without. *Philos Trans R Soc Lond B Biol Sci* **371**, 1-8, doi:10.1098/rstb.2015.0506 (2016).
- 6 Dickey, S. W., Cheung, G. Y. C. & Otto, M. Different drugs for bad bugs: antivirulence strategies in the age of antibiotic resistance. *Nat Rev Drug Discov* **16**, 457-471, doi:10.1038/nrd.2017.23 (2017).
- 7 Johnson, B. K. & Abramovitch, R. B. Small molecules that sabotage bacterial virulence. *Trends Pharmacol Sci* **38**, 339-362, doi:10.1016/j.tips.2017.01.004 (2017).
- 8 Koul, A. *et al.* Cloning and characterization of secretory tyrosine phosphatases of *Mycobacterium tuberculosis*. *J Bacteriol* **182**, 5425-5432 (2000).
- 9 Chauhan, P. *et al.* Secretory phosphatases deficient mutant of *Mycobacterium tuberculosis* imparts protection at the primary site of infection in guinea pigs. *PloS one* **8**, e77930, doi:10.1371/journal.pone.0077930 (2013).
- 10 Singh, R. *et al.* Disruption of mptpB impairs the ability of *Mycobacterium tuberculosis* to survive in guinea pigs. *Mol Microbiol* **50**, 751-762 (2003).
- 11 Beresford, N. *et al.* MptpB, a virulence factor from *Mycobacterium tuberculosis*, exhibits triple-specificity phosphatase activity. *Biochem J* **406**, 13-18, doi:10.1042/BJ20070670 (2007).
- 12 Di Paolo, G. & De Camilli, P. Phosphoinositides in cell regulation and membrane dynamics. *Nature* **443**, 651-657, doi:10.1038/nature05185 (2006).
- 13 Beresford, N. J. *et al.* Inhibition of MptpB phosphatase from *Mycobacterium tuberculosis* impairs mycobacterial survival in macrophages. *J Antimicrob Chemother* **63**, 928-936, doi:10.1093/jac/dkp031 (2009).
- 14 Zhou, B. *et al.* Targeting mycobacterium protein tyrosine phosphatase B for antituberculosis agents. *Proc Natl Acad Sci U S A* **107**, 4573-4578, doi:10.1073/pnas.0909133107 (2010).
- 15 Dutta, N. K. *et al.* Mycobacterial protein tyrosine phosphatases A and B inhibitors augment the bactericidal activity of the standard anti-

- tuberculosis regimen. *ACS Infect Dis* **2**, 231-239, doi:10.1021/acsinfecdis.5b00133 (2016).
- 16 Grundner, C., Ng, H. L. & Alber, T. Mycobacterium tuberculosis protein tyrosine phosphatase PtpB structure reveals a diverged fold and a buried active site. *Structure* **13**, 1625-1634, doi:10.1016/j.str.2005.07.017 (2005).
- 17 Grundner, C. *et al.* Structural basis for selective inhibition of Mycobacterium tuberculosis protein tyrosine phosphatase PtpB. *Structure* **15**, 499-509, doi:10.1016/j.str.2007.03.003 (2007).
- 18 Vidal, D., Blobel, J., Perez, Y., Thormann, M. & Pons, M. Structure-based discovery of new small molecule inhibitors of low molecular weight protein tyrosine phosphatase. *Eur J Med Chem* **42**, 1102-1108, doi:10.1016/j.ejmech.2007.01.017 (2007).
- 19 Vidal, D., Thormann, M. & Pons, M. A novel search engine for virtual screening of very large databases. *J Chem Inf Model* **46**, 836-843, doi:10.1021/ci050458q (2006).
- 20 Tanaka, A. *et al.* Inhibitors of acyl-CoA:cholesterol O-acyltransferase. 2. Identification and structure-activity relationships of a novel series of N-alkyl-N-(heteroaryl-substituted benzyl)-N'-arylureas. *Journal of medicinal chemistry* **41**, 2390-2410, doi:10.1021/jm9800853 (1998).
- 21 Potkin, V. I., Petkevich, S. K., Lyakhov, A. S. & Ivashkevich, L. S. Mononuclear heterocyclic rearrangement of 5-arylisoazole-3-hydroxamic acids into 3,4-substituted 1,2,5-oxadiazoles. *Synthesis-Stuttgart* **45**, 260-264, doi:10.1055/s-0032-1317947 (2013).
- 22 Melo, T. M. V. D. P. E., Lopes, C. S. J., Gonsalves, A. M. D. R. & Storr, R. C. Reactivity of 2-halo-2H-azirines. Part II. Thermal ring expansion reactions: Synthesis of 4-haloisoxazoles. *Synthesis-Stuttgart*, 605-608 (2002).
- 23 Watterson, S. H. *et al.* Potent and Selective Agonists of Sphingosine 1-Phosphate 1 (S1P(1)): Discovery and SAR of a novel isoxazole based series. *Journal of medicinal chemistry* **59**, 2820-2840, doi:10.1021/acs.jmedchem.6b00089 (2016).
- 24 Schnettger, L. *et al.* A Rab20-dependent membrane trafficking pathway controls M. tuberculosis replication by regulating phagosome spaciousness and integrity. *Cell Host Microbe* **21**, 619-628 e615, doi:10.1016/j.chom.2017.04.004 (2017).
- 25 Flynn, J. L. Lessons from experimental Mycobacterium tuberculosis infections. *Microbes Infect* **8**, 1179-1188, doi:10.1016/j.micinf.2005.10.033 (2006).
- 26 Helke, K. L., Mankowski, J. L. & Manabe, Y. C. Animal models of cavitation in pulmonary tuberculosis. *Tuberculosis (Edinb)* **86**, 337-348, doi:10.1016/j.tube.2005.09.001 (2006).
- 27 Jain, R. *et al.* Enhanced and enduring protection against tuberculosis by recombinant BCG-Ag85C and its association with modulation of cytokine profile in lung. *PloS one* **3**, e3869, doi:10.1371/journal.pone.0003869 (2008).
- 28 Beresford, N. J., Saville, C., Bennett, H. J., Roberts, I. S. & Taberner, L. A new family of phosphoinositide phosphatases in microorganisms:

- identification and biochemical analysis. *BMC Genomics* **11**, 457, doi:10.1186/1471-2164-11-457 (2010).
- 29 Kastner, R. *et al.* LipA, a tyrosine and lipid phosphatase involved in the virulence of *Listeria monocytogenes*. *Infect Immun* **79**, 2489-2498, doi:10.1128/IAI.05073-11 (2011).
- 30 Vaughan, W. R. & Spencer, J. L. 5-Phenyl-2-isoxazoline-3-carboxylic acid. *J Org Chem* **25**, 1160-1164, doi:Doi 10.1021/Jo01077a022 (1960).
- 31 King, G. S., Rzepa, H. S. & Magnus, P. D. Reductive and oxidative cleavage of 5-phenyl-delta-2-isoxazoline-3-carboxylic acid. *J Chem Soc Perk T 1*, 437-443, doi:Doi 10.1039/P19720000437 (1972).
- 32 Dannhardt, G. *et al.* Regioisomeric 3-aminomethyl, 4-aminomethyl and 5-aminomethyl isoxazoles - synthesis and muscarinic activity. *Eur J Med Chem* **30**, 839-850, doi:Doi 10.1016/0223-5234(96)88303-6 (1995).
- 33 Lindsay-Scott, P. J., Clarke, A. & Richardson, J. Two-step cyanomethylation protocol: convenient access to functionalized aryl- and heteroarylacetonitriles. *Org Lett* **17**, 476-479, doi:10.1021/ol503479g (2015).
- 34 Morris, G. M. *et al.* AutoDock4 and AutoDockTools4: Automated docking with selective receptor flexibility. *J Comput Chem* **30**, 2785-2791, doi:10.1002/jcc.21256 (2009).
- 35 Vidal, D., Thormann, M. & Pons, M. LINGO, an efficient holographic text based method to calculate biophysical properties and intermolecular similarities. *J Chem Inf Model* **45**, 386-393, doi:10.1021/ci0496797 (2005).
- 36 Bifani, P. J. *et al.* Origin and interstate spread of a New York City multidrug-resistant *Mycobacterium tuberculosis* clone family. *JAMA* **275**, 452-457 (1996).
- 37 Mosmann, T. Rapid colorimetric assay for cellular growth and survival: application to proliferation and cytotoxicity assays. *J Immunol Methods* **65**, 55-63 (1983).

Table of Contents graphic

